Virginia Commonwealth University
VCU Scholars Compass

Theses and Dissertations | Graduate School

2022

Targeting BCL-2 Family Proteins In Therapy Induced Senescent Cancer Cell Models

Wade Cook
Virginia Commonwealth University

Follow this and additional works at: https://scholarscompass.vcu.edu/etd

Part of the Cellular and Molecular Physiology Commons, Molecular Biology Commons, Oncology Commons, and the Other Chemicals and Drugs Commons

© The Author

Downloaded from
https://scholarscompass.vcu.edu/etd/7164

This Thesis is brought to you for free and open access by the Graduate School at VCU Scholars Compass. It has been accepted for inclusion in Theses and Dissertations by an authorized administrator of VCU Scholars Compass. For more information, please contact libcompass@vcu.edu.

TARGETING BCL-2 FAMILY PROTEINS IN THERAPY INDUCED SENESCENT CANCER CELL MODELS

A thesis submitted in partial fulfillment of the requirements for the degree of Master of Science at Virginia Commonwealth University

By

Wade J. Cook
James Madison University, B.S. 2016

Director: Hisashi Harada, Ph.D.
Philips Institute for Oral Health Research
VCU School of Dentistry

Virginia Commonwealth University
Richmond, VA
November 2022

Acknowledgements

I would first like to acknowledge my mentor Dr. Hisashi Harada. Thank you so much for everything you have done for me over the past few years and allowing me to be a part of your lab. Each time I have decided to pursue a different career you have welcomed me back into your lab and given me guidance whenever possible. Your dedication to cancer research is inspiring.

I would also like to thank my managers at Pharmaceutical Product Development (PPD). When I first pitched the idea of attaining a masters degree while continuing to work full-time you guys offered me nothing but unwavering support and you worked with me to come up with a schedule that would accommodate my educational endeavors. I am sincerely grateful for your patience and understanding over the past year.

To my committee members, Dr. Roland Pittman and Dr. Yue Sun. Thank you for volunteering your time to be on my committee and for offering constructive feedback on my project. You pushed me to better understand my project and I feel I got more out of it because of that.

To my lab members. Victoria Neely, Kissanet Birhane, Khanh Nguyen, Colette Creamer, Natalie Luffman, and Casey Sheehy. Thank you so much for offering your time to train me on techniques and for helping me out with some procedures when I wasn't at VCU.

To my family…Dad, Mom, brothers, sister. Thanks for continuing to check in on me throughout the process and feigning interest in my project. It's been a wild ride.

Finally, to my awesome fiancé Victoria Riss. Thank you so much for everything you do. You have been there for me for the past year and I know I couldn't have finished this up without you.

Table of Contents

1 Background and Introduction:

1.1 Cancer……8

1.2 Non-Small Cell Lung Cancer……...11

1.3 Head and Neck Squamous Cell Carcinoma……14

1.4 Diagnosis and Treatment……19

1.5 Apoptosis……23

1.6 BCL-2 Family Proteins……26

1.7 Therapy-Induced Cellular Senescence……29

1.8 Senolytics……31

2 Specific Aims

2.1 Determine the Senolytic Capabilities of AZD-4320 Compared with the Senolytic Capabilities of ABT-263……33

2.2 Determine if the Senolytic Capabilities of AZD-4320 Translate into an *in vivo* Mouse Model……34

3 Materials and Methods

3.1 Cell Lines and Cell Culture……34

3.2 WST1 Assay……35

3.3 Crystal Violet Staining……35

3.4 Apoptosis Assay via Annexin V/PI Staining……..36

3.5 β-Galactosidase Staining ……36

3.6 Immunoblotting……37

3.7 Mouse Xenograft, Tumor Generation, and Treatment……38

3.8 Tumor Measurement, Extraction, and Fixation……...38

3.9 Statistical Analyses……..39

4 Results and Discussion

4.1 HNSCC/NSCLC Cell Lines and Therapeutic Agents……40

4.2 Optimal Dosage of Cisplatin to Induce Senescence in Cancer Cell Lines…….41

4.3 Cisplatin Does Induce Senescence in Both HNSCC and NSCLC……..42

4.4 Combination Therapy of Cisplatin Followed by Dual BCL-X_L/BCL-2 Inhibitors, ABT-263 or AZD-4320, Significantly Reduces Viability of HNSCC and NSCLC Cells……43

4.5 ABT-263 and AZD-4320 Are Just as Effective as Combinational Treatment with ABT-199 + A1155463……..47

4.6 Cisplatin Increases Gene Expression of the Anti-Apoptotic Proteins BCL-X_L and/or BCL-2 and Combination Cisplatin + AZD-4320 Has a Synergistic Effect……..48

4.7 Observing Cell Viability with Cisplatin and Combination Treatment Using Florescence Activated Cell Sorting……..51

4.8 Determining the Effectiveness of Cisplatin + AZD-0466 Combination Treatment in a MOC Mouse Xenograft Model……..52

4.9 Pilot Study to Determine if CMT or LLC is a Better Candidate for NSCLC Mouse Xenograft Model……55

4.10 Determining the Senolytic Capabilities of AZD-0466 in an LLC Mouse Xenograft Model……57

List of Figures

Scheme 1: Stages of Cancer…….10

Scheme 2: Anatomical Location of NSCLC……12

Scheme 3: Scheme 3: Layout of *TP53* gene showing mutation hotspots due to inhalation of tobacco smoke……..14

Scheme 4: Anatomical Location of HNSCC……16

Scheme 5: General Cell Cycle Diagram Showing G1/S Checkpoint……...18

Scheme 6: The Intrinsic Pathway of Apoptosis……26

Scheme 7: Layout of the BCL-2 Homology Domains for Members of the BCL-2 Family Proteins……..28

Scheme 8: Mode of Action of BH3-Mimetics……...33

Scheme 9: Measuring Mouse Tumors Using Digital Caliper……39

Figure 1: WST1 Cell Proliferation Assays……41

Figure 2: β-galactosidase Staining……43

Figure 3: Crystal Violet Staining……...45

Figure 4: Crystal Violet Staining to Determine Effectiveness of Dual BCL-2/BCL-X_L Inhibitors……47

Figure 5: Western Blot Analysis……50

Figure 6: Fluorescence Activated Cell Sorting Analysis of MOC1……52

Figure 7: MOC1 Mouse Xenograft Study using C57BL/6 Mice……..54

Figure 8: MOC1 C57BL/6 Mouse IVIS imaging……55

Figure 9: CMT167/LLC Mouse Xenograft Pilot Study Using C57BL/6 Mice……56

Figure 10: LLC Mouse Xenograft Study Using C57BL/6 Mice……..60

Conclusion

References

Abbreviations

ALK: Anaplastic Lymphoma Kinase
Apaf-1: Apoptosis Protease Activating Factor-1
BCL-2: B-Cell Lymphoma 2
BCL-X_L: B-Cell Lymphoma Extra Large
BAK: BCL-2 Homologous Antagonist Killer
BAX: BCL-2 Associated X Protein
BAD: BCL-2 Associated Agonist of Cell Death
BH: BCL-2 Homology
BID: BH3 Interacting Domain Death Agonist
BIM: BCL-2 Interacting Mediator of Cell Death
CAF: Cancer-Associated Fibroblasts
CDK4: Cyclin Dependent Kinase 4
CDK6: Cyclin Dependent Kinase 6
CDKI: Cyclin-Dependent Kinase Inhibitors
CTL: Cytotoxic T Lymphocytes
CTLA4: Cytotoxic T-Lymphocyte Antigen 4
DISC: Death-Inducing Signaling Complex
DMEM: Dulbecco's Modified Eagle Medium
DNA: Deoxyribose nucleic Acid
EGF: Epidermal Growth Factor
EGFR: Epidermal Growth Factor Receptor
FACS: Florescence Activated Cell Sorting
FBS: Fetal Bovine Serum
FDA: Food and Drug Administration
HNSCC: Head and Neck Squamous Cell Carcinomas
HPV: Human Papillomavirus
IACUC: Institution Animal Care and use Committee
IVIS: *In vivo* Imaging System
LLC: Lewis Lung Cancer
MAGE-A3: Melanoma-Associated Antigen-A3
MCL-1: Myeloid Cell Leukemia 1
NK: Natural Killer
NNK: Nicotine-Derived Nitrosamine Ketone
NOXA: "Latin for damage"
NSCLC: Non-Small Cell Lung Cancer
OIS: Oncogene-Induced Senescence
PAH: Polycyclic Aromatic Hydrocarbons
PBS: Phosphate Buffered Saline
PD1: Programmed Cell Death 1
PUMA: p53 Upregulated Modulator of Apoptosis
PRIMA-1: p53 Re-Activation and Induction of Massive Apoptosis
Rb: Retinoblastoma-Associated Protein
ROS: Reactive Oxygen Species
RPMI: Roswell Park Memorial Institute
RS: Replicative Senescence
RT: Room Temperature
SASP: Senescence Associated Secretory Phenotype
SCLC: Small Cell Lung Cancer
SNP: Single-Nucleotide Polymorphisms
TAM: Tumor-Associated Macrophages
TCGA: The Cancer Genome Atlas
TIS: Therapy-Induced Senescence
TKR: Tyrosine Kinase Receptors
TME: Tumor Microenvironment
TNFR: Tumor Necrosis Factor Receptor
4NQO: 4-nitroquinoline-1 oxide

Abstract

TARGETING BCL-2 FAMILY PROTEINS IN THERAPY INDUCED SENESCENT CANCER CELL MODELS

Non-small Cell Lung Cancer (NSCLC) originates from numerous different cell types in the lungs and is among the deadliest of cancers. Head and Neck Squamous Cell Carcinomas (HNSCC) are derived from the mucosal membranes of the oral cavity, pharynx, and larynx. Both NSCLC and HNSCC are predominately caused by tobacco smoke inhalation and as such mutations in the tumor suppressor gene *TP53* are common. Since similarities exist in the root cause of NSCLC and HNSCC, they may also share similarities in treatment methods. Cisplatin is a platinum-based DNA damaging agent that has been used as a cancer chemotherapy for decades. While highly effective in the eradication of cancer cells, cisplatin also causes severe toxicity to patients when given in high doses. Previous research has shown that treatment with lower dosages of cisplatin can induce cancer cells into a state of senescence. In this state, the cancer cells are in growth arrest but remain metabolically active. Unfortunately, senescent cancer cells display a SASP (senescence associated secretory phenotype) that causes a prolonged inflammatory response in patients. The SASP is associated with angiogenesis and metastasis of the cancer cells. In addition, it has been shown that cancer cells can escape senescence and in doing so become more drug resistant and aggressive. A current field of cancer research involves selectively eradicating cancer cells that have first been induced into senescence using cisplatin or other traditional chemotherapies. Drugs that were once used to inhibit specific protein targets in the cancer cells are being repurposed as senolytics. The central idea of inducing cancer cells into senescence is that specific protein targets become upregulated upon treatment with cisplatin. The anti-apoptotic proteins BCL-X_L and BCL-2 are two key proteins that promote cancer cell survival after exposure to DNA-damaging agents such as cisplatin. Once these proteins become overexpressed in the cancer cells, they make perfect targets for a class of drugs that act as BCL-X_L and BCL-2 inhibitors. Previously research has shown that the dual BCL-X_L/BCL-2 inhibitor ABT-263 is effective at selectively eradicating cancer cells that have been induced into senescence. However, ABT-263 was unable to pass clinical trials as it was shown to cause dose-limiting thrombocytopenia. Thrombocytopenia is a condition of low platelet counts in the blood. This is because platelets rely on BCL-X_L for survival. For this reason, a new BCL-X_L/BCL-2 inhibitor was formulated known as AZD-4320. AZD-4320 works in a similar manner to ABT-263 and only causes transient thrombocytopenia that can be managed. Here we show that AZD-4320 is a potent senolytic agent and is effective at eradicating both HNSCC and NSCLC cells *in vitro* and *in vivo*.

Background and Introduction:

1.1 Cancer:

Cancer is a broad term used to describe a group of more than 100 diseases that involve the uncontrolled proliferation of cells in the body. This uncontrolled division is due to the fact that cancer is able to evade the stringent regulatory systems in normal cells that controls their growth and reproduction. Normal functioning cells, go through a cell cycle in which they proliferate to make new daughter cells. This process is mainly controlled by two categories of genes; proto-oncogenes and tumor-suppressor genes (National Institutes of Health, 2007). Proto-oncogenes encode proteins that stimulate cell division and inhibit apoptosis, or programmed cell death. Tumor-suppressor genes, on the other hand, inhibit cell proliferation. In the cell, there exists a delicate balance between the expression of proto-oncogenes and tumor suppressor genes and this allows cells to develop and proliferate at normal frequencies. Disruptions in this homeostatic balance, caused by mutations in both proto-oncogenes and tumor-suppressor genes, is the basis for cancer development (Chial, 2008).

Accumulated mutations in cancer cells causes changes to their genetic makeup making them more prolific and less predictable compared to healthy cells. Normal cells generally need a cell matrix to grow on, as well as interaction with other cells and tissue components. They also require extrinsic growth factors to stimulate their growth and proliferation. Cancer cells, on the other hand, express fewer cell adhesion molecules making them more mobile and less reliant on a cell matrix or cell-to-cell interactions. In addition, some cancerous cells can also produce their own growth factors, which allows them to grow perpetually. It is these unique properties of cancer that make them so dangerous as they are able to migrate, invade surrounding tissue, and eventually, metastasize (Cooper, 2000).

Metastasis is the process whereby cancerous cells enter the circulatory or lymphatic system and translocate to different regions of the body. This process begins with angiogenesis and lymphangiogenesis whereby cancer cells secrete growth factors to signal the formation of new blood and lymph vessels, respectively. As a cancer grows it requires a higher volume of oxygen and nutrients from the bloodstream to survive. During metastasis, cancer cells secrete proteases that digest the extracellular matrix, which forms the barrier between epithelial cells and endothelial cells of capillaries and lymph vessels. Next, the cancer cells invade into the circulatory system or lymphatic system to access nutrients and spread to different regions of the body (Cooper, 2000).

There are five stages used to classify the severity of a particular cancer (Scheme 1). Stage 0, indicates carcinoma *in situ*, meaning the tumor size is small and it has not spread from where it originated. Generally, cancers in Stage 0 are considered pre-cancerous and are easily treatable. Stage I, cancer is similar to Stage 0, however, the cancer has continued to grow in size. Stage II, the cancer has continued to grow and is larger than in Stage I, however, it still has not spread to other tissues or lymph nodes. Stage III, the cancer has advanced enough to invade surrounding lymph nodes. Finally, Stage IV, is metastatic cancer (Rosen, 2022).

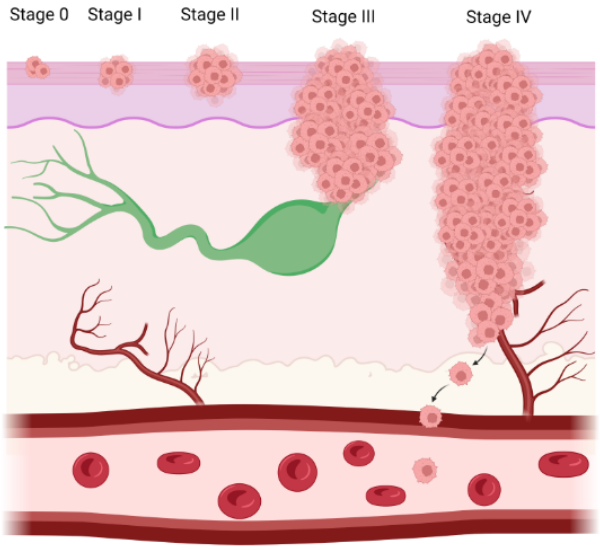

Created with biorender.com

Scheme 1: Stages of Cancer
Stage 0) Carcinoma *in situ*, pre-cancerous
Stage 1) Carcinoma has grown in size but not spread
Stage 2) Carcinoma has grown larger than Stage 1, but has not spread to tissue or lymph nodes
Stage 3) Carcinomas has grown passed Stage 2, and may have invades lymph nodes
Stage 4) Metastatic cancer

Most cancers are categorized into four main groups based on the type of cell in which they originate. Carcinomas arise from mutations in epithelial cells. Sarcomas are rarer and materialize as solid tumors in connective tissues, such as muscle, bone, cartilage, and fibrous tissues. Leukemias occur in blood forming cells, and lymphomas occur in cells of the immune system. Carcinomas are the most prevalent cancer and account for approximately 90% of all cases (Cooper, 2000).

Cancer is the second leading cause of death in the United States following heart disease. Analysis by the American Cancer Society, estimates that 1,918,030 new cancer cases are projected in the US alone in the year 2022. Risk factors for the development of cancer include: diet, age, obesity, genetic predisposition, viral infection, and exposure to carcinogens (Siegel,

2022). Notably, carcinogens found in tobacco smoke have been estimated to be responsible for nearly one-third of all cancer related deaths (Cooper, 2000).

1.2 Non-Small Cell Lung Cancer (NSCLC):

Non-Small Cell Lung Cancer (NSCLC) is among the deadliest of cancers, with over 50% patient mortality within a year of diagnosis (Zappa, 2016). NSCLC makes up about 85% of all lung cancers with Small Cell Lung Cancer (SCLC) accounting for the remaining 15%. The main risk factor for the development of lung cancer is cigarette smoke with 90% of lung cancers being attributed to smoking. Before the 20th century, lung cancer was a relatively rare disease. However, with the increased usage of cigarettes and other tobacco products, the rates of lung cancer have soared in recent decades (Siddiqui, 2022).

There are three main subtypes of NSCLC: squamous cell carcinoma, adenocarcinoma, and large cell carcinoma. The different subtypes of lung cancer relate to their area of origin within the lung (Scheme 2). Squamous Cell Carcinoma arises from epithelial cells located in bronchioles in the center of the lungs and is highly correlated with smoke inhalation. Adenocarcinomas originate in type II alveolar cells, which are glandular cells and secrete mucous in the periphery of the airways (Zappa, 2016). Adenocarcinomas are the most common subtype of lung cancer, accounting for around 40% of all diagnoses, and are the most common lung cancer in nonsmokers. The final subtype of lung cancer is known as Large Cell Carcinomas. Less is known about this subtype and generally it is diagnosed when the other two subtypes have been ruled out. Large Cell Carcinomas are usually found in the periphery of the lung in cells that are not of squamous or glandular origin (Tai, 2020).

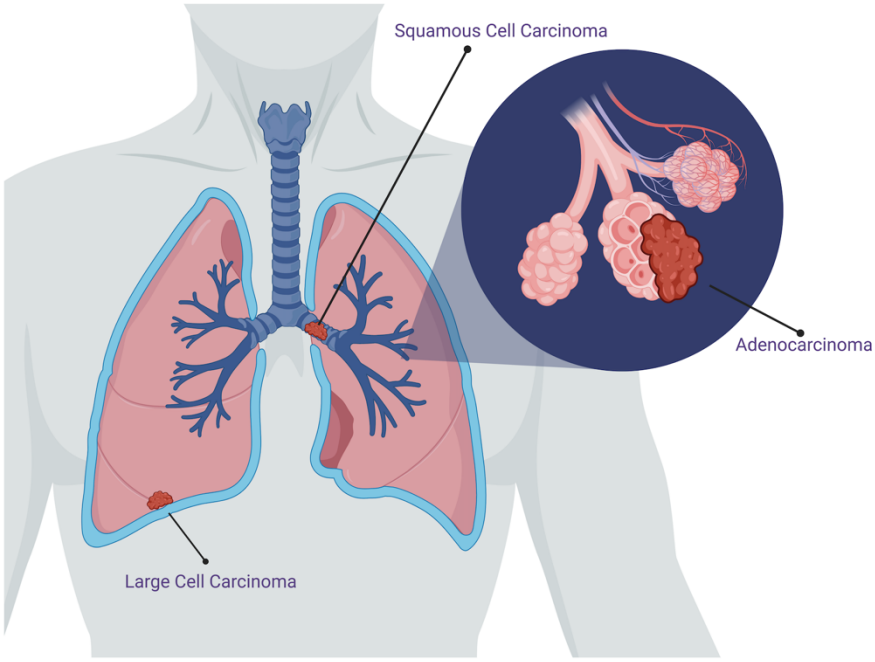

Created with biorender.com

Scheme 2: Anatomical Location of NSCLC
Squamous cell carcinoma arises from epithelial cells located in the bronchioles. Adenocarcinomas arise from mucous secreting type II alveolar cells. Large cell carcinomas are located in the periphery of the lungs in cells that are not of squamous or glandular origin.

By and large the greatest contributor to NSCLC diagnosis is cigarette smoke. However, there are a number of environmental and occupational hazards that have been linked to NSCLC as well. Radon has been identified as the second leading cause of lung cancer and the primary risk factor for nonsmokers. It is a natural carcinogen and is a product of the radioactive decay of uranium-238. The main sources of indoor radon contamination include: soil around housing foundations, building materials, fuels, and domestic water (Li, 2020). In addition, inhalation of commercial and industrial arsenic derived products such as insecticides, herbicides, and wood preservers are associated with increased lung cancer incidence. Finally, living in large

metropolitan areas with sustained exposure to vehicle emissions containing polycyclic aromatic hydrocarbons (PAH) has been associated with an 8% increased risk of lung cancer mortality (Zappa, 2016).

There are some links to a genetic predisposition to lung cancer and nicotine dependence, however, these mechanisms are poorly understood as they are masked by the overwhelming influence of environmental factors. Recently, six separate genetic studies comprising a total of 4,502 lung cancer cases along with 7,377 control cases from several European Countries, found single-nucleotide polymorphisms (SNP) on chromosome 15 in regions that code for three different nicotinic acetylcholine receptor subunits (*CHRNA5, CHRNA3,* and *CHRNA4*). SNPs in this region were associated with a 14% increased risk of lung cancer development and they are passed from parent to offspring. These subunits are expressed in alveolar epithelial cells, pulmonary neuroendocrine cells, and lung cancer cell lines. Additionally, these subunits have been shown to specifically bind *N'-nitrosonornicotine*, a class I carcinogen produced in the processing of tobacco, and potentially other carcinogens (Hung, 2008).

In the late 1980s, it was discovered that lung tumors have exceptionally high rates of mutations in the tumor suppressor gene *TP53*. This gene encodes the p53 protein which plays a protective role in regulation of the cell cycle by binding to DNA, eliciting a series of events that inhibit cell division. Once mutated, p53 is unable to effectively bind DNA and the "stop signal" it provides to the cell cycle is abolished. This causes uncontrolled cell growth resulting in tumorigenesis. Genomic studies carried out by The Cancer Genome Atlas (TCGA) have shown that lung adenocarcinomas and squamous cell carcinomas have a mutated p53 rate of 46% and 81%, respectively. This high rate of p53 mutation is mainly due to the thousands of carcinogens in tobacco smoke. Nicotine-derived nitrosamine ketone (NNK) and PAH are two well

documented carcinogens in tobacco smoke and cause mainly guanine to thymine transversions in the *TP53* gene. Interestingly, there are four main mutation hotspots within the *TP53* DNA-binding domain that code for amino acids V157, R175, R248, and R273. Mutations in the DNA-binding domain have a dramatic effect on p53's ability to bind DNA and exert its tumor suppressive effects (Gibbons, 2014) (Scheme 3).

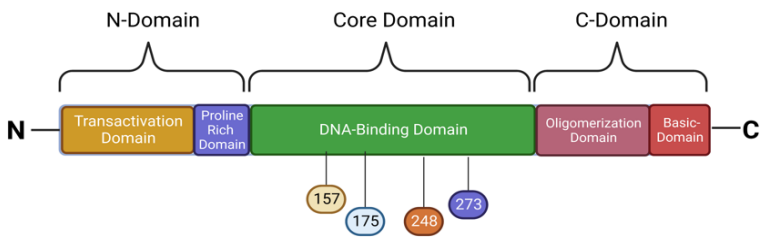

Created with biorender.com

Scheme 3: Layout of *TP53* gene showing mutation hotspots due to inhalation of tobacco smoke
Tobacco smoke inhalation is a well-known carcinogen. In NSCLC it causes mutations in the *TP53* gene in four well document hotspots that code for the amino acids V157, R175, R248, and R273. These mutations are located in the DNA-binding domain of the *TP53* gene and lead to a non-functional p53 protein, incapable of binding DNA and exerting its tumor-suppressive effects.

1.3 Head and Neck Squamous Cell Carcinoma (HNSCC):

Head and Neck Squamous Cell Carcinomas (HNSCC) are the sixth most common cancer worldwide and account for approximately 350,000 deaths per year (Vigneswaran, 2014). HNSCC is usually classified into two groups based on the root cause of the disease; HPV-positive and HPV-negative HNSCC. HPV-positive HNSCC is primarily due to infection by an oncogenic strain of the human papillomavirus (HPV). HPV-negative HNSCC, on the other hand, is primarily due to the consumption of carcinogen containing products such as alcohol and tobacco. Interestingly, the incidence of HPV-negative HNSCC varies from country to country, mainly due to cultural and demographical differences in modifiable risk behaviors. For example,

areas of Southeast Asia and Australia have a high prevalence of HNSCC due to the increased consumption of alcohol and tobacco products. Whereas India, Taiwan, and some provinces of mainland China have higher rates of oral cavity cancer due to the chewing of areca nut, a local plant seed believed to be helpful for the digestive system. Alternatively, the USA and Western Europe have seen a rise in HPV-positive HNSCC due to increased transmission of the human papilloma virus, which is primarily transmitted through oral sex. The incidence of HNSCC is increasing year over year and it is anticipated that there will be a 30% increase in HNSCC cases by the year 2030 (Johnson, 2020).

HNSCC is derived from mucosal epithelium in the oral cavity, pharynx, and larynx. Generally, tobacco use and excessive alcohol consumption are the main causes of cancer development in the oral cavity and larynx, while cancer of the pharynx is increasingly being linked to infection by HPV (Scheme 4). More than 70% of oropharyngeal cancers are linked to HPV infection, with HPV-16 being the most oncogenic strain. It is possible to discern whether the origin of a particular HNSCC was due to HPV infection or not by observing the gene expression of the cancer. HPV-positive HNSCC has distinct gene expression and mutation profiles that differentiate it from HPV-negative HNSCC (Johnson, 2020).

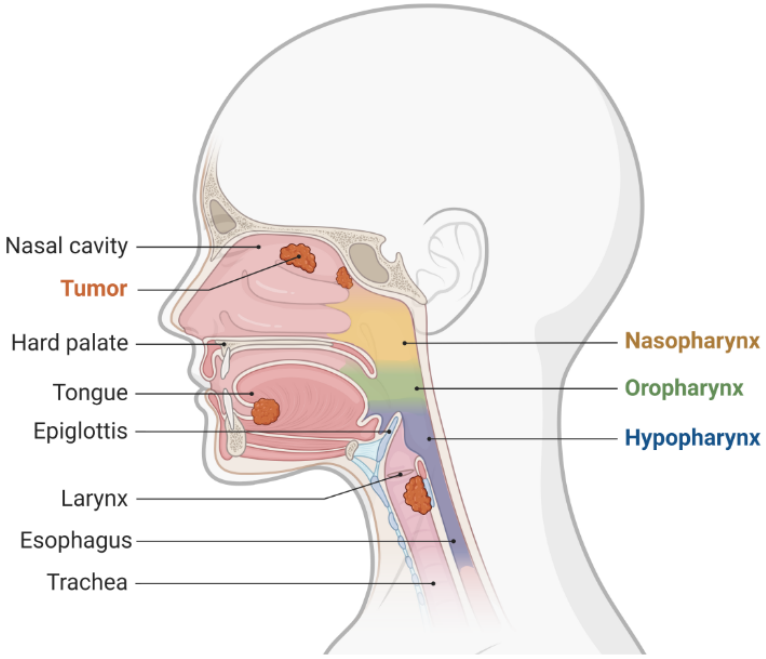

Created with biorender.com

Scheme 4: Anatomical Location of HNSCC
HNSCC is derived from mucosal epithelium of the oral cavity, pharynx, and larynx. Cancer in the oral cavity and larynx is generally attributed to excessive tobacco and alcohol use, while cancer in the pharynx is largely attributed to infection with HPV-16.

HPV-16 is a small, double-stranded DNA virus responsible for the majority of HPV-positive HNSCC. It's meager 7,900 base pair genome consists of 8 protein-encoding genes and 2 noncoding regions (Cornet, 2012). Two proteins of interest are E6 and E7, as they are essential for oncogenic transformation of the host cell. E6 promotes the ubiquitination and eventual degradation of the tumor suppressor protein p53. E7 promotes the degradation of retinoblastoma-associated protein (Rb), an important regulatory protein for the cell cycle (Johnson, 2020). Rb inhibits the transition from the G1-phase to the S-phase of the cell cycle, a key checkpoint that commits the cell to division. Together the viral proteins E6 and E7 disrupt the host cell's ability to regulate its own division resulting in uncontrolled growth.

As mentioned above, HPV-negative HNSCC is almost entirely caused by the consumption of alcohol or use of tobacco products. Furthermore, there is evidence that simultaneous alcohol and tobacco use can have a synergistic effect increasing likelihood for the onset of carcinogenesis. Carcinogens from alcohol and tobacco most commonly cause mutations in the tumor suppressor genes *CDKN2A* (22% of tumors) and *TP53* (72% of tumors). *CDKN2A* codes for the protein p16 which inhibits Cyclin Dependent Kinase 4 (CDK4) and Cyclin Dependent Kinase 6 (CDK6). CDK4 and CDK6 phosphorylate Rb thereby inactivating it and promoting G1 to S-phase transition. *CDKN2A* mutation leads to non-functional p16 enabling the continued phosphorylation of Rb by CDK4 and CDK6 promoting cell division (Johnson, 2020) (Scheme 5). While similar mechanisms underlie the tumorigenic properties of both HPV-positive and HPV-negative HNSCC, there is a key distinction which allows discernment between the two cancers. In HPV-negative HNSCC, frequent exposure to carcinogens results in mutated genes. In HPV-positive HNSCC, proteins, the functional products of the genes, are degraded. This variation has led to different therapeutic approaches for HPV-negative and HPV-positive HNSCC.

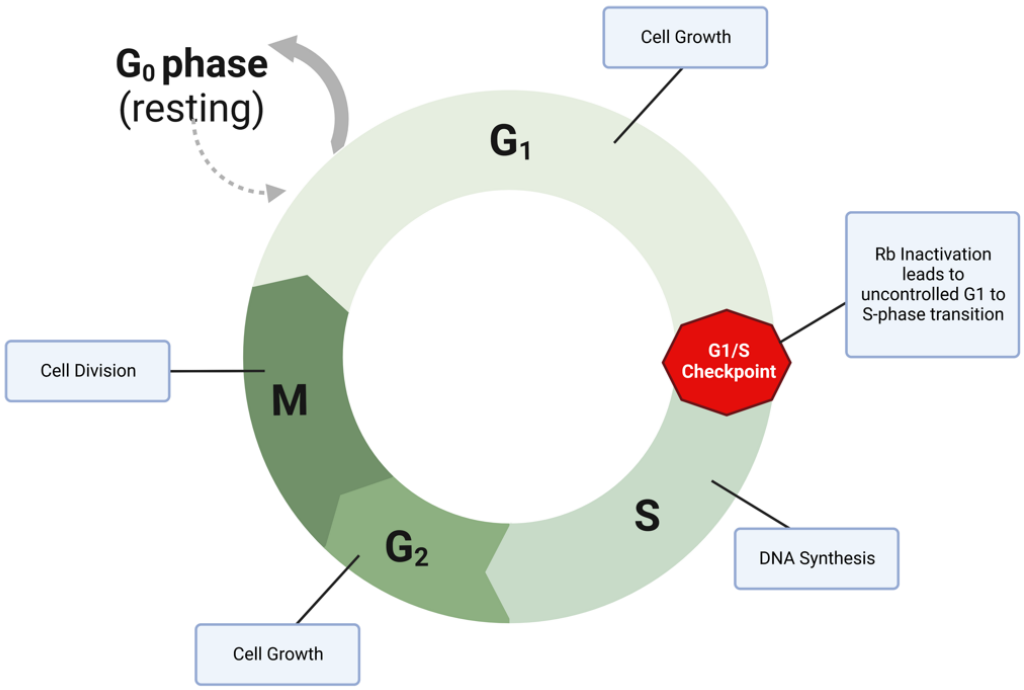

Created with biorender.com

Scheme 5: General Cell Cycle Diagram Showing G1/S Checkpoint
The G1/S checkpoint is an important step in the mediation of cell proliferation. This checkpoint is highly regulated by the Rb protein. When Rb is phosphorylated by CDK4 and CDK6, it is inactivated and is unable to regulate G1/S phase transition leading to uncontrolled cell proliferation. *CDKN2A* is a gene that encodes the p16 protein which inactivates CDK4 and CDK6. It is often mutated in HNSCC leading to increased activation of CDK4 and CDK6 and therefore, increased inactivation of Rb.

An emerging field of study in the treatment of HNSCC is focusing not only on the cancer cells themselves, but on the interactions between the cancer cells and their environment. The tumor microenvironment (TME) is a complex mixture of cancer cells and stromal cells including endothelial cells, cancer-associated fibroblasts (CAF), and immune cells (Johnson, 2020). Advanced cases of HNSCC show increased numbers of tumor-associated macrophages (TAM) and mast cells. Mast cells are white blood cells that interact with endothelial cells to stimulate the formation of new blood vessels. Recruited TAMs locally secrete epidermal growth factor (EGF) which draw the cancer cells towards blood vessels by chemotaxis. Both mast cells and

TAMs are involved in angiogenesis. CAFs are the most abundant cell type observed in the tumor microenvironment and secrete proteases that breakdown the extracellular matrix (Kootongkaew, 2013). This helps the cancer cells penetrate blood vessels and metastasize to other regions of the body. By shifting focus to the TME, researchers may be able to slow down cancer invasion and metastasis leading to significantly better patient outcomes.

1.4 Diagnosis & Treatment:

With today's current medicine, the five-year survival rate of NSCLC is 17.5%, while HNSCC has a better prognosis of roughly 60% (Zappa, 2016 and Reyes-Gibby, 2014). Prophylactic measures are the most important step to take to reduce the overall morbidity of both NSCLC and HNSCC. This includes modifying risky behaviors, such as tobacco and alcohol consumption, that lead to the onset of the diseases. In addition to prophylaxis, there are several routes to therapy including: surgery, radiation, immunotherapy, and chemotherapy. In many cases, a combination of some or all of these therapies is necessary to help eliminate the cancer.

NSCLC Therapy:

One reason for the reduced survival rate of NSCLC is due to late diagnosis. Generally, patients are unaware that they have NSCLC and approximately 40% of all NSCLC cases are first diagnosed at stage IV (Zappa, 2016). If diagnosed before stage IV, surgical removal of a lobe or section of the lung is usually the best option. However, if diagnosed at stage IV or beyond, the first line of treatment is usually administration of a combination of cytotoxic chemotherapeutic agents.

One commonly used chemotherapy in NSCLC patients is receptor tyrosine kinase inhibitors. Tyrosine kinase receptors (TKR) are responsible for many functions in the cell

including cell proliferation, and TKR genes are commonly mutated in cancer. Epidermal Growth Factor Receptor (EGFR) is a cell-surface tyrosine kinase receptor that, when mutated, remains constitutively activated leading to uncontrolled cell growth. NSCLC patients with mutated EGFR have shown a 70% response rate to the FDA-approved tyrosine kinase inhibitors, Erlotinib and Gefitinib. Anaplastic Lymphoma Kinase (ALK) is another receptor tyrosine kinase that is mutated in 3-7% of all lung tumors. It shows no response to either Erlotinib or Gefitinib, however, patients have shown a 50-61% response rate to Crizotinib, an FDA-approved tyrosine kinase inhibitor (Zappa, 2016). Due to the variations in each individual case of NSCLC, personalized medicine routines that focus on targeting and mitigating the effects of specific genetic mutations have shown the best patient outcomes.

In addition to targeting TKRs, which increase the proliferation of cancer cells, there is also interest in restoring the tumor-suppressive activities of p53. One agent known as PRIMA-1 (p53 re-activation and induction of massive apoptosis) was developed as a possible remedy to restore wild-type function to the mutated p53 protein (Gibbons, 2014). As stated before, mutations in the DNA-binding domain of the *TP53* give rise to an altered p53 protein, incapable of effectively binding DNA. PRIMA-1 is capable of stabilizing p53 leading to increased transcription of many of its target genes including *NOXA, PUMA,* and *BAX* (Gibbons, 2014). These genes are involved in promoting apoptosis and their upregulation has been shown to increase cell cycle arrest and cell death.

Immunotherapies are an emerging field in cancer treatment and focus on using the body's own defense systems to eradicate tumor cells. Since cancer cells originate from the body's healthy cells, it is often difficult for the immune system to recognize when cancer pathology has begun. In addition, cancerous cells actively down-regulate the immune response by modulating

the activity of T-cells in the body. The Cytotoxic T-Lymphocyte Antigen 4 (CTLA4) and Programmed Cell Death 1 (PD1) receptors are involved in the down-regulation of the immune system by cancer cells. Both PD1 and CTLA4 overexpression leads to reduced T-cell activation and proliferation. As such, two monoclonal antibodies were developed, Ipilimumab and Nivolumab, that specifically target and mitigate the functions of CTLA4 and PD1, respectively (Zappa, 2016). Studies have shown some increase in immune response when patients are treated with these immunotherapies and both Ipilimumab and Nivolumab received FDA-approval for the treatment of metastatic or recurrent NSCLC in May 2020 (Vellanki, 2021).

In addition to the development of monoclonal antibodies to inhibit specific immune suppressing targets, the advent of cancer vaccines is an up-and-coming field in cancer immunotherapy. There are several methods employed in the development of cancer vaccines that help the body recognize when healthy cells have turned cancerous. Belagenpumatucel-L (Lucanix) uses genetically modified whole tumor cells that stimulate T-cell activation specifically against NSCLC. Another method uses alterations in the gene expression of NSCLC to specifically target these cells for destruction. Two proteins, Melanoma-Associated Antigen-A3 (MAGE-A3) and the membrane associated glycoprotein MUC1, are overexpressed specifically in NSCLC cells (Zappa, 2016). Tumor vaccines have been employed that bind MAGE-A3 and MUC1 and target them for destruction by the body's immune system. None of these vaccines have been FDA-approved and they are currently in ongoing clinical trials.

HNSCC Therapy:

In stark contrast to NSCLC, HNSCC is usually diagnosed early and as such has a much better prognosis. Depending on the location of HNSCC, the onset of different symptoms generally leads to awareness of disease progression. Oral cavity tumors usually present as an

unhealing lesion leading to pain when speaking. Laryngeal tumors are often associated with hoarseness of the voice. HPV-negative oropharyngeal tumors usually present as pain when swallowing or ear pain, while HPV-positive oropharyngeal tumors most commonly present as a painless mass in the neck (Johnson, 2020).

Surgery is most often employed for small primary tumors that are localized with limited transition to lymph nodes. Cure rates for surgical interventions in HNSCC of this type is around 80%. Surgical intervention is most commonly elected for oral cavity tumors due to ease of access, while laryngeal or pharyngeal tumors are often treated using radiation therapy. If the cancer has progressed to the lymph nodes a combination of post-operative radiation and chemotherapy are recommended to reduce the recurrence of HNSCC (Johnson, 2020).

Cisplatin is a commonly used chemotherapy in HNSCC and is generally administered concurrently with radiotherapy. Cisplatin is a platinum-based DNA damaging agent that, once administered, covalently binds to the purine bases guanine and adenine. This leads to breaking of the DNA strand and eventual apoptosis of the cell. While cisplatin does not distinguish between healthy human cells and cancerous cells, it is particularly effective at neutralizing rapidly dividing cells as there is an increased rate of DNA replication in these cells (Le, 2018). This makes it most effective in tumors that behave more aggressively. In addition, to its ability to cause cellular apoptosis, cisplatin has been shown to have a radio-sensitizing effect, increasing the efficiency of radiotherapy (Johnson, 2020).

A main deterrent to the use of high-dosage cisplatin is its cytotoxic effects. In fact, cisplatin is currently only FDA-approved for the treatment of advanced ovarian, testicular, and bladder cancers. All other uses of cisplatin are “off-label” and are usually only prescribed when the benefits outweigh the significant potential for adverse effects. Cisplatin is known to cause

nephrotoxicity, peripheral neuropathy, severe nausea and vomiting, and myelosuppression (Le, 2018).

In order to improve patient outcomes and quality of life, new chemotherapeutic agents such as cetuximab are being researched. Cetuximab is an FDA-approved monoclonal antibody against EGFR. Much like NSCLC, EGFR is overexpressed in almost all instances of HNSCC, making it a good target for therapy. Importantly, cetuximab has been shown to have lower toxicity than cisplatin. To date, cetuximab in combination with radiotherapy was shown to have similar patient outcomes as cisplatin with radiotherapy in HPV-negative HNSCC patients. However, HPV-positive HNSCC patients benefited more from cisplatin in combination with radiotherapy (George, 2014).

In addition to the above chemotherapies, similar immunotherapies being researched in NSCLC are being implemented in HNSCC. Pembrolizumab is an FDA-approved immune checkpoint inhibitor that targets PD1. HNSCC patients with high PD1 expression benefited from administration of pembrolizumab, while patients with low PD1 expression and severe symptoms benefited from a combination of pembrolizumab and a platinum-based chemotherapy. Along with pembrolizumab, Nivolumab is FDA-approved for the treatment of both NSCLC and HNSCC (Georges, 2014).

As research efforts continue, the main goal in HNSCC therapy is to mitigate the adverse effects of platinum-based chemotherapies such as cisplatin to improve patient outcomes.

1.5 Apoptosis:

Apoptosis is a complex and highly orchestrated process in which cells undergo distinct morphological changes that ultimately lead to cellular death. Hallmarks of apoptosis include

chromatin condensation, nuclear fragmentation, rounding of the cell and reduction in cellular volume (Wong, 2011). Apoptosis is a natural process that occurs during development, aging, and maintaining cell populations in the body (Elmore, 2007). In cancer, the delicate balance between natural cell division and cell death becomes dysregulated leading to uncontrolled cellular proliferation. Activating apoptosis specifically in cancer cells has become a vehicle for treatment in recent decades.

There are two main pathways of apoptosis; the intrinsic or mitochondrial pathway and the extrinsic or death receptor pathway. While these pathways differ mechanistically, they both converge at a single point called the execution pathway, after which the cell is destined to undergo apoptosis. The execution pathway is initiated by the cleavage of caspase-3, a cysteine protease, and as such caspase-3 is a common indicator protein for the onset of apoptosis (Wong, 2011). Caspase-3 belongs to a family of proteins most of which are expressed in an inactive zymogen form known as procaspases. Once enzymatically cleaved, procaspases become activated caspases and a caspase cleaving cascade begins ultimately resulting in apoptosis.

The main distinction between the intrinsic and the extrinsic pathways is how they are initiated. The extrinsic pathway is initiated by pro-death signals from outside the cell, usually from Natural Killer (NK) cells or CD8-Positive Cytotoxic T Lymphocytes (CTL) (Cusick, 2022). The process begins when a “death receptor”, such as a tumor necrosis factor receptor (TNFR), expressed on the outside of a target cells binds a soluble ligand or ligand expressed on the surface of an immune cell such as a NK or CTL. TNF receptors are part of a superfamily of proteins involved in the transduction of “death signals” from the outside of the cell into intracellular death signals. Once TNF binds to TNFR, the pro-apoptotic protein FADD is recruited and binds to the “death domain” of the TNF receptor on the inside of the cell

membrane. Together these proteins form the death-inducing signaling complex (DISC), which recruits procaspase 8 (Wong, 2011). Procaspase 8 is then cleaved and is able to activate caspase 3 leading to a caspase cascade involving caspases 3, 6, and 7 and eventually apoptosis.

The intrinsic pathway is non-receptor mediated and involves the activation of intracellular signals that eventually lead to pore formation in the mitochondria and release of cytochrome C, a protein that normally functions in the mitochondrial respiratory chain. The intrinsic pathway can be activated by various factors including UV radiation, oxidative stress, hypoxia, chemotherapeutic agents, and DNA damage. Once cytochrome C is released from the mitochondria, it attaches to the cytosolic adaptor protein apoptosis protease activating factor-1 (Apaf-1). The cytochrome C/Apaf-1 complex recruits pro-caspase 9 to form the apoptosome. Once formed, procaspase-9 undergoes self-cleavage and initiates the activation of the executioner caspases 3,6, and 7 leading to apoptosis (Scheme 5). Of note are proteins in the B-Cell Lymphoma 2 (BCL-2) family, which regulate the intrinsic pathway of apoptosis (Elmore, 2007).

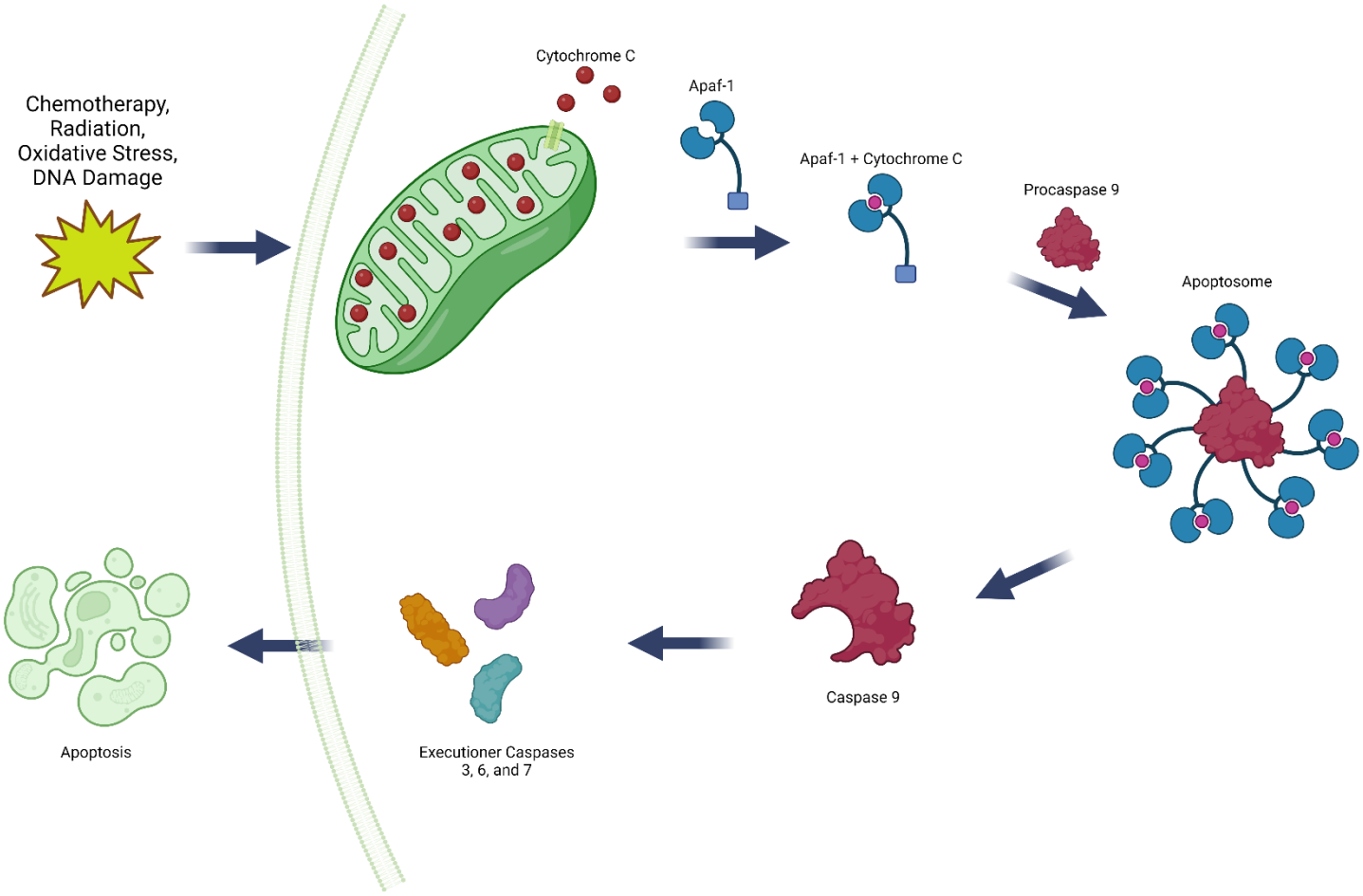

Created with biorender.com

Scheme 6: The Intrinsic Pathway of Apoptosis
The intrinsic pathway of apoptosis is non-receptor mediated and is activated by UV radiation, oxidative stress, hypoxia, chemotherapeutic agents, and DNA damage. Once the cell is damaged, pores are formed in the mitochondria and cytochrome C is released. It binds to cytosolic Apaf-1 and the cytochrome C/Apaf-1 complex recruits pro-caspase 9, forming the apoptosome. Pro-caspase 9 then undergoes self-cleavage and activates the executioner caspases 3, 6, and 7 leading to apoptosis.

1.6 BCL-2 Family Proteins:

The BCL-2 gene family consists of approximately 20 proteins involved in the regulation of the intrinsic pathway of apoptosis. Often times, the expression of BCL-2 family proteins is deregulated in oncogenic cells leading to a reduction in apoptosis and resistance to

chemotherapies. BCL-2 family proteins can be subdivided into two categories, pro-apoptotic proteins (BIM, BID, BAD, PUMA, and NOXA) and anti-apoptotic proteins (BCL-2, BCL-X_L, and MCL-1). Two other proteins that are important in the BCL-2 family are the effector proteins BAK and BAX. Upon activation, BAX and BAK oligomerize to form pores in the mitochondrial outer membrane, releasing cytochrome C, resulting in the caspase cascade that leads to apoptosis (Kale, 2018).

Since activation of BAK and BAX is fatal to the cell, they are kept under extremely stringent regulation by the anti-apoptotic proteins BCL-2, BCL-X_L, and MCL-1. These three proteins are able to neutralize the effects of BAK and BAX, through binding, and thus, inactivation of their effects in the cell. BCL-2, BCL-X_L, and MCL-1 contain four conserved BCL-2 Homology (BH) domains (BH1-4), while BAK and BAX contain three conserved BH domains (BH1-3). In contrast, the pro-apoptotic proteins BIM, BAD, PUMA, and NOXA only contain the BH3 domain, and as such, they are aptly categorized as BH3-only proteins (Scheme 6). These BH3 only proteins promote apoptosis in two ways. First, they can antagonize the interaction of BAK and BAX to the antiapoptotic proteins allowing the release and subsequent activation of BAK and BAX. This is the mode of action for BAD, NOXA, and PUMA. Second, they are able to directly bind to and activate BAK and BAX. This is the mode of action for BID and BIM. It is the interaction of the BH3 domain between the members of the pro-apoptotic proteins and anti-apoptotic proteins that inevitably determines the induction of apoptosis in the cell (Kale, 2018).

In the cell, BAX is located in the cytoplasm and when activated by BIM migrates to the mitochondria. BAK is located on the mitochondrial outer membrane and is selectively activated by BID. Once activated, BAX and BAK can form pores in the mitochondria in two ways. BAX

or BAK can oligomerize independently and form homodimers in the mitochondrial outer membrane. Alternatively, BAK and BAX can interact together and form heterodimers. In either circumstance, the outcome is the same and cytochrome C is released from the mitochondria leading to apoptosis.

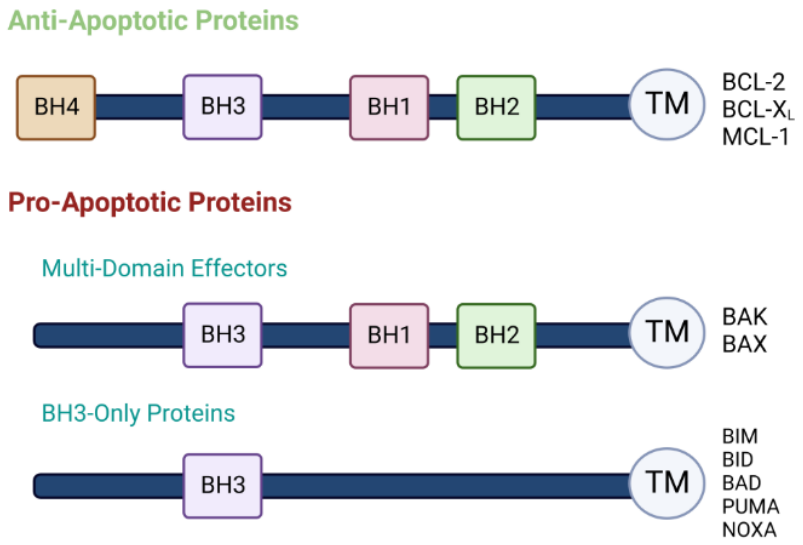

Created with biorender.com

Scheme 7: Layout of the BCL-2 Homology Domains for Members of the BCL-2 Family Proteins The anti-apoptotic proteins BCL-2, BCL-X_L, and MCL-1 contain four BH domains BH1 – BH4. The pro-apoptotic effectors BAK and BAX contain three BH domains BH1 – BH3. Finally, the pro-apoptotic BH-3 only proteins BIM, BID, BAD, PUMA, and NOXA contain only the BH3 domain. The anti-apoptotic proteins mitigate the apoptosis inducing effects of the pro-apoptotic proteins through binding of their BH3 domain, thus inactivating them.

In cancer, the expression of the anti-apoptotic proteins BCL-2, BCL-X_L, and MCL-1 is often upregulated. This effectively inhibits apoptosis as the abundance of anti-apoptotic proteins sequesters the majority of the pro-apoptotic proteins through binding of their BH3 domain. In addition, overexpression of BCL-2, BCL-X_L, and MCL-1 generally confers chemoresistance as the intrinsic pathway is inhibited by high expression of these proteins. Therefore, inhibition of the anti-apoptotic proteins is of key interest in the development of novel cancer therapies.

1.7 Therapy-Induced Cellular Senescence:

Cellular senescence is a state in which cells cease to divide but remain metabolically active. It was first observed *in vitro* in 1961 when serially passaged cells reached a point where they underwent extensive morphologic and phenotypic changes that resulted in growth arrest (Pawlikowski, 2013). This was the first evidence to suggest that human cell lines have a finite lifespan, mostly due to the telomere attrition associated with successive replication cycles. This form of senescence is termed replicative senescence (RS) and has been associated with the aging process in humans. Another form of senescence can be triggered by the activation of oncogenes, termed oncogene-induced senescence (OIS). Furthermore, exposure to prolonged stressors including DNA damage and reactive oxygen species (ROS) can also cause cells to enter a state of senescence. Senescence is a protective mechanism that is activated when cells are exposed to both exogenous or endogenous stressors, however, it also plays a role in a variety of different biological processes including wound healing and embryonic development (van Deursen, 2014).

Senescence is a contradictive process, and may play a role in both tumor-suppression and tumor-progression. Cells in OIS increase the expression of the cyclin-dependent kinase inhibitors (CDKI) p16 and p21, as well the master regulatory protein p53. As mentioned before, p16 inhibits CDK4 and CDK6 mitigating their ability to phosphorylate and inactivate Rb. P21 is transcriptionally regulated by p53 and is responsible for inhibiting CDK2, another CDK that phosphorylates and inactivates Rb leading to uncontrolled G1/S phase transition. Therefore, growth arrest is maintained in senescent cells through upregulation of the p21/p53 and p16/Rb pathways. This is an important tumor-suppressive strategy to avoid replication of potentially oncogenic cells. Conversely, senescence can also lead to tumor progression. A hallmark of senescence is the senescence associated secretory phenotype (SASP). Senescent cells secrete a

host of proteins including: inflammatory molecules (e.g. interleukins, cytokines, and chemokines) growth factors, and proteases. The release of interleukins, cytokines, and chemokines elicits an immune response drawing immune cells to the site of inflammation. While immune cells can be helpful in the elimination of cancerous cells, certain immune cells in the TME are involved in angiogenesis. Furthermore, the release of proteases from senescent cells can degrade the ECM leading to invasion and metastases of cancer cells. Current evidence suggests that acute senescence is ideal for tumor-suppression but a prolonged SASP can result in tumor-progression (Pawlikowski, 2013).

Therapy-Induced Senescence (TIS) is a novel tool being utilized in the field of cancer therapy. It was previously thought that the best treatment options for patients was complete destruction of cancer cells by high dosage cytotoxic compounds or high dose radiation. However, these treatments are often associated with severe side effects that sometimes outweigh the benefits of therapy. It was discovered that using certain cytotoxic compounds at a lower dosage was enough to induce cancer cells into a senescent state with limited adverse side effects. For example, cisplatin and doxorubicin (a DNA damaging agent) are two cytotoxic agents used to induce senescence. It is important to note that while both of these drugs are capable of inducing apoptosis at higher concentrations, lower dosages only induce growth arrest. While p21 and p16 are normally upregulated in senescent cells, *CDKN2A* (gene encoding p16) and p53 (transcription factor for p21) are commonly mutated in both NSCLC and HNSCC. However, it has been shown that cancer cells with mutated p53 and/or mutated *CKDN2A* can still be induced into senescence using cytotoxic agents and radiotherapy (Ewald, 2010).

The current gold standard in the detection of senescent cells *in vitro* is the use of β-galactosidase staining. Cells that have been induced into a senescent state display an enlarged,

flattened morphology as well as heightened activity of the lysosomal β-galactosidase. X-gal is a synthesized substrate for the β-galactosidase, that when cleaved, stains blue. It has been shown that treatment with low dosage cisplatin or doxorubicin over a period of days is enough to induce cells into senescence and stain blue when treated with X-gal.

1.9 <u>Senolytics:</u>

Previous research has suggested that senescence is a permanent state of growth arrest. However, there is recent evidence that suggests cancer cells can escape senescence and become more aggressive and therapy resistant in a post-senescent state (Ahmadinejad, 2021). Therefore, it is imperative that once a cancerous population is induced into senescence by cytotoxic agents it should be targeted for destruction to decrease harm from the SASP and minimize the potential of escape from senescence.

Senolytic agents are a class of drugs that were developed to specifically target and destroy cells in senescence. TIS changes the gene expression of cells in a predictive manner that can be exploited using senolytic agents. Cancer cells that have been treated with a low dosage of cisplatin often overexpress the anti-apoptotic proteins BCL-X_L and BCL-2. As previously mentioned, rapidly dividing cancer cells are more prone to the DNA-damaging effects of cisplatin and upregulate BCL-X_L and BCL-2 in order to prevent apoptosis. Several senolytic agents have been identified that act as inhibitors of BCL-X_L and BCL-2. This inhibition disrupts the interaction between the anti-apoptotic proteins BCL-X_L and BCL-2 and pro-apoptotic BAX and BAK. These inhibitors are aptly named BH3 mimetics.

The therapeutic potential of BH3 mimetics was first unveiled with the development of the BCL-2/BCL-X_L dual inhibitor ABT-263 (Navitoclax). Selective targeting of the BH3 domain of

BCL-2 and BCL-X_L allows for the release of pro-apoptotic proteins followed by the activation of the effector protein BAX/BAK and eventual BAX/BAK oligomerization. This leads to pore development in the mitochondrial outer membrane, release of cytochrome C, and apoptosis. Unfortunately, it has been established that BCL-X_L is a primary survival factor of platelets. Inhibition of BCL-X_L leads to a rapid decrease in circulating platelets leading to the potentially fatal condition known as thrombocytopenia. This led to the development of the BCL-2 selective inhibitor ABT-199 (Venetoclax). While selective inhibition of BCL-2 mitigates the onset of thrombocytopenia, cancers with high expression of MCL-1 or BCL-X_L confers resistance to Venetoclax (Souers, 2013). Another single target inhibitor A-1155463 was developed to inhibit BCL-X_L alone, and while effective, this also resulted in the onset of thrombocytopenia in murine models (Tao, 2014). Currently, the BCL-2/BCL-X_L dual inhibitor AZD-4320 is being researched as a potential senolytic agent. Here I show that AZD-4320 is a potent inducer of apoptosis in therapy-induced senescent cell models with high BCL-2/BCL-X_L expression. Furthermore, while AZD-4320 does cause thrombocytopenia, it is transient and generally resolves within a week.

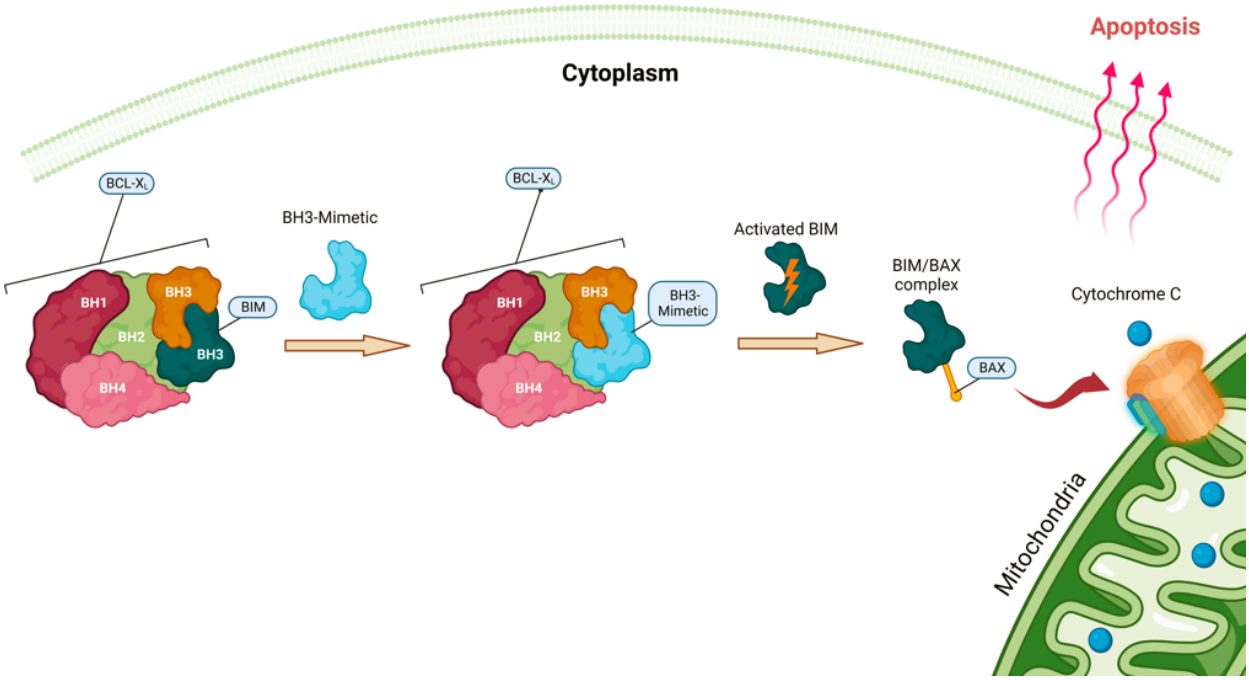

Created with biorender.com

Scheme 8: Mode of Action of BH3-Mimetics
BH3 mimetics antagonize the interaction of the pro-apoptotic proteins with anti-apoptotic proteins. BAD, NOXA, and PUMA antagonize the interaction of BAX and BAK with either BCL-2 or BCL-X_L. BID and BIM directly activate BAK and BAX, respectively. In the above scenario, the BH3 mimetic antagonizes the interaction of BIM with BCL-X_L. Once released, BIM is activated and is able to activate BAX. BAX migrates to the mitochondria where it oligomerizes with other BAX and/or BAK proteins. BAX/BAK homodimers and heterodimers form pores in the mitochondrial outer membrane, resulting in cytochrome C release and eventual apoptosis.

Specific Aims

2.1 Determine the Senolytic Capabilities of AZD-4320 Compared with ABT-263

It has been established that ABT-263 is a potent senolytic agent. We aim to show that AZD-4320 is as potent or more potent than ABT-263 in combination with cisplatin. We show the potency of AZD-4320 through crystal violet staining, western blot analysis, and FACS.

2.2 Determine if the Senolytic Capabilities of AZD-4320 Translate into an *in vivo* Mouse Model

We want to determine if AZD-4320 works as a senolytic in an immune competent live animal model. C57BL/6 mice were inoculated with several different HNSCC and NSCLC cell lines. Tumor growth and response to therapy was monitored.

Materials and Methods:

3.1 Cell Lines and Cell Culture:

Non-Small Cell Lung Cancer Murine Cell Lines, CMT167 and LLC (Lewis Lung Carcinoma) were used. CMT167 was isolated from an alveogenic lung carcinoma of a C57BL/6 mouse, while LLC was established by inoculation with a primary Lewis Lung Carcinoma into a C57BL/6 mouse. Head and Neck Squamous Cell Carcinoma Murine Cell Lines MOC1 and 602 were used. MOC1 originates from the oral cavity. 602 was established by Ahmadinejad *et al* at Virginia Commonwealth University and was derived from a 4-nitroquinoline-1 oxide (4NQO)-developed tumor on the tongue. Both MOC1 and 602 were transfected with the Luciferase gene using lentivirus-mediated transfection. CMT167, 602, and MOC1 were cultured in DMEM 1x Medium (Thermo Fisher Scientific) and supplemented with 10% fetal bovine serum (FBS) and 100 ug/mL penicillin/streptomycin (Thermo Fisher Scientific). LLC was cultured in RPMI 1x Medium (Thermo Fisher Scientific) and supplemented with 10% FBS and 100 ug/mL penicillin/streptomycin (Thermo Fisher Scientific). LLC also required the use of poly-D-lysine in the cell culture dish in order for the cells to better adhere. Poly-D-lysine plates were made by applying a 1:1 mixture of poly-D-lysine and PBS to the cell culture dish, letting it sit for an hour, and then rinsed with DI water. All cell lines were routinely treated with Normocyin to prohibit mycoplasma contamination. Additionally, MOC1 and 602 were routinely treated with puromycin

to select for progeny that contained the transfected Luciferase gene. Cultures were maintained in a humidified incubator at 37 deg C and 5% CO2.

3.2 WST1 Assay:

Cells were seeded in triplicate in a 96-well plate at a density of $1x10^4$ cells/well. 24 hours post-seeding, cells were treated with a titration of cisplatin at concentrations of 0.5 µM, 1 µM, 2 µM, 5 µM, 10 µM, 20 µM, and 50 µM. DMSO was used as a control. 3 wells consisted of only culture medium to account for background absorbance. Three days post-treatment, 10 µL WST1 reagent was added to each well. After 2 – 3 hours, a color change was visualized and the absorbance was measured at 450 nm. The mean of each triplicate was calculated and the background absorbance was subtracted out for the different concentrations of cisplatin.

3.3 Crystal Violet Staining:

Cells were seeded into 6-well plates based on their relative doubling speeds. MOC1 was seeded with 5×10^4 cells/well, 602 and CMT were seeded with 1×10^5 cells/well, and LLC was seeded with 2×10^5 cells/well. Cells were then treated with cisplatin based on their relative sensitivities to the chemotherapeutic agent; MOC1 (7.5 uM), 602 (2.5 uM), CMT (10 uM), and LLC (2.5 uM). Cells were then treated with a vehicle (DMSO) or 1uM of a senolytic agent: AZD-4320 (AstraZeneca), ABT-263 (AbbVie), ABT-199 (ApexBio), or A-1155462 (ApexBio). 24h after treatment, medium was aspirated, cells were washed with Phosphate Buffered Saline (PBS) and fixed with cold methanol for 15 minutes. Fixative was removed and crystal violet staining solution (0.05% v/v) was applied to cells and left to incubate at room temperature (RT) for 30 minutes. Staining solution was removed, and wells were rinsed with distilled water three to four times and left to dry.

3.4 Apoptosis Assay by Annexin-V and Propidium Iodide Staining:

Moc1 cells were divided into four treatment groups (control, AZD-4320, cisplatin, and combination cisplatin + AZD-4320). Cells in the cisplatin treatment groups were seeded (5 x 10^4 cells/plate) into 6 cm dishes; triplicates for each condition. These cells were then treated with 7.5 uM cisplatin and left to incubate for five days. Cells in the control and AZD-4320 groups were treated with a vehicle (DMSO) and 0.2 uM AZD-4320, respectively, and left to incubate for 48 hours. Supernatant was removed and transferred to labeled conical tubes. Remaining adherent cells were trypsinized using 500 uL 0.25% Trypsin-EDTA and added to the appropriate conical tubes. Cells were centrifuged at 1,000 rpm for five minutes and the supernatant was removed. Cell pellets were washed with 1 mL of cold PBS and resuspended in 100 uL of 1x Binding Buffer (10 mM HEPES (pH 7.4), 140 mM NaCl, and 2.5 mM CaCl2). Each sample received 10uL propidium iodide (Sigma Aldrich) and 3 uL of Annexin V (BioLegend). Samples were lightly vortexed and incubated in the dark for 15 minutes at RT, and 400 uL of 1x Binding Buffer was added to the final suspension. Samples were analyzed by flow cytometry (BD FACSCanto).

3.5 Beta-Galactosidase Staining:

Growth media was removed from the 6-well plate. Each well was washed with 2 mL of 1x cold PBS. 1 mL of cold fixative solution (2% Formaldehyde, 0.2% Glutaraldehyde, 97% 1x PBS) was applied and allowed to fix for 15 minutes at RT. Plates were rinsed two times with 1x PBS. 1mL of B-Galactosidase Staining Solution (Cell Signaling: 1% 100x solution A, 1% 100x solution B, 5% 20mg/mL x-gal solution, 93% 1x staining solution) was added to each well. Plates were wrapped with parafilm and incubated at 37% overnight in a dry incubator. Cells were

imaged the following day under a microscope (200x total magnification). For storage of plates, B-Galactosidase Staining Solution was removed from the plates and 1mL of 70% glycerol was applied to cells and stored at 4 deg C.

3.6 Immunoblotting:

Adherent cells were scraped from cell culture dishes, transferred into a conical tube and centrifuged at 1,000 rpm for five minutes. Supernatant was removed and the pellet was washed with 1 mL cold PBS and transferred to an Eppendorf tube. The washed lysates were centrifuged at 8000 x G for 2 minutes. PBS was aspirated and whole cell lysates were prepared with lysis buffer [1:200 ratio of protease inhibitor cocktail, 1:100 ratio of phosphatase inhibitor cocktails 2 and 3 (Sigma-Aldrich, St.Louis, MO)]. Lysates were left on ice for 15-20 minutes, centrifuged at 15,000 x G for five minutes at 4 deg C and the supernatant was transferred to a labeled tube. Protein concentrations were determined using the Bradford method and a spectrophotometer (Bio-Rad, Hercules, CA). Equal amounts of sample were loaded into SDS-polyacrylamide gels. The samples were run at 180 V for 55 minutes and transferred onto nitrocellulose membranes (Fisher Scientific, Pittsburg, PA) at 100 V for 60 minutes. Membranes were submerged in a blocking agent (5% evaporated skim milk and 0.1% Tween-20 in 1x PBS) for 30 minutes. Membranes were cut based on molecular weight. Appropriate primary antibodies were applied with blocking agent at a concentration of 1:1000 and incubated overnight at 4 deg C. Membranes were washed in PBS-T (0.1% Tween-20 in 1x PBS) three times for five minutes each and then incubated with appropriate secondary antibodies (HRP-linked anti-rabbit IgG or anti-mouse IgG) for one hour at RT. Membranes were washed with PBS-T for ten minutes and developed using ECL-2 Western Blotting Substrate (Thermo Fisher Scientific).

3.7 Mouse Xenograft Tumor Generation and Treatment:

To test the senolytic capabilities of AZD-0466 (AZD-4320-dendrimer conjugate) on tumor growth in mouse xenograft models, cells were collected in their respective growth media, spun down at 1,000 rpm for five minutes and washed with cold PBS. PBS was aspirated and cells were resuspended in a mixture of Matrigel and cold PBS in a 1:1 ratio. For the orthotopic injections, $1x10^5$ cells suspended in 50 μL of PBS-matrigel mixture were orthotopically injected in the left cheek of the C57BL mice. For the rear flank injections, $1x10^6$ cells were suspended in 100 μL of PBS-matrigel mixture and injected into the left rear flank. Once tumors developed to a palpable size (around one-week post-injection), tumors were measured and the mice were randomized into different treatment groups so that the average size of the tumors in each group was more or less equal when treatment started. Cisplatin was administered by intraperitoneal injection at a dosage of 5 mg/kg, once a week for two weeks. AZD-0466 was administered by tail vein injection at a dosage of 100 mg/kg once a week until the study was terminated. Mice were euthanized once the tumor size reached the humane endpoint according to IACUC policy. If the tumor was ulcerated, prevented adequate eating/hydration, or mice exhibited signs of declining conditions. Euthanasia was performed by CO_2 asphyxiation followed by cervical dislocation.

3.8 Tumor Measurements, Extraction, and Fixation:

Tumor growth was monitored every other day, measured twice a week using a digital caliper, and detected using IVIS imaging once a week. Tumor volume was determined using the formula $V = (W^2 \times L)/2$, where L was the length in mm and W was the width in mm. Following

euthanasia of mice, tumors were excised, removing fascia, hair, and epidermal layers, and fixed in 25 mL of formalin.

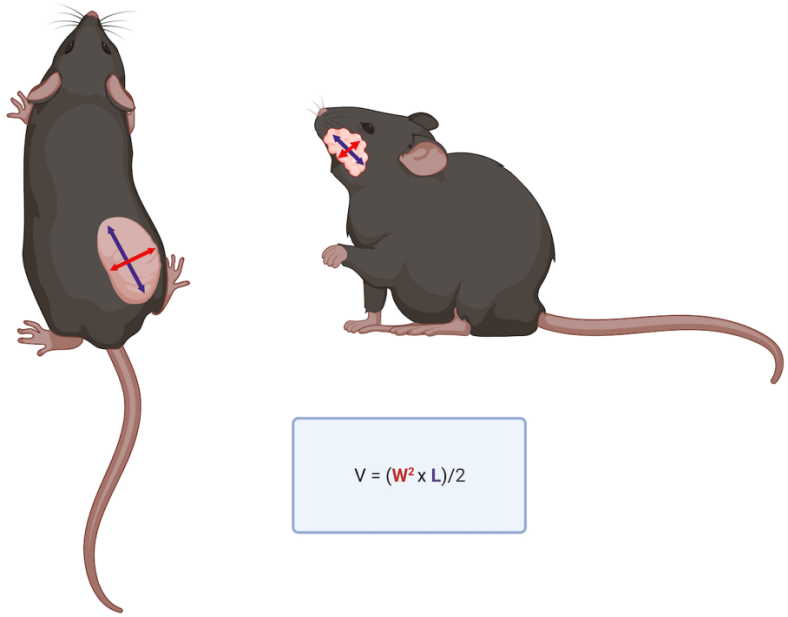

Created with biorender.com

Scheme 9: Measuring Mouse Tumors Using Digital Caliper
The mouse tumors were measured with length (L) being the longest part of the tumor and width (W) being the shorter part of the tumor. Tumor volume was then calculated using the formula $V = (W^2 \times L)/2$

3.9 Statistical Analyses:

The graphs presented were made and statistical analyses were performed using Microsoft Excel 2019 software. Standard error was calculated by dividing the standard deviation by the population sizes square root. A standard paired, two-tailed, T-test was used to determine P-values and $p < 0.05$ was considered statistically significant.

Results and Discussion:

4.1 HNSCC/NSCLC Cell Lines and Therapeutic Agents

Four mouse cell lines were used to determine the efficacy of numerous senolytic agents. CMT167 and LLC were derived from mouse lung tumors and were used as a NSCLC models. MOC1 and 602 were derived from mouse tumors in the head and neck and were used a HNSCC models. While NSCLC and HNSCC display distinct phenotypes, there are some similarities between the two diseases. Both are associated with the respiratory system and are inextricably linked to the use of tobacco products. As such, there is a high incidence of p53 mutations in both diseases. Due to these similarities, there may be overlapping modes of therapies that are effective against both NSCLC and HNSCC.

Cisplatin is a commonly used chemotherapy in several types of cancer. Cells treated with cisplatin undergo severe DNA damage due to the cross-linking of purine bases, resulting in double strand breaks. Cisplatin is particularly effective against cancer cells due to their rapid division and DNA synthesis. However, there are several side effects associated with cisplatin treatment including: myelosuppression, immunosuppression, nephrotoxicity, and neurotoxicity. In addition, many cancers either acquire resistance to cisplatin over time or are intrinsically resistant. As such, higher doses of cisplatin are required to treat these cancers which can result in severe organ toxicity (Florea, 2011).

In an effort to reduce toxicity and overcome drug resistance, cisplatin in combination with other agents is currently being investigated. One current strategy is using a low dosage of cisplatin to induce cells into senescence, followed by subsequent treatment with a senolytic

agent. We compared the senolytic capabilities of the following drugs: ABT-263 (Navitoclax), ABT-199 (Venetoclax), A-1155463, and AZD-4320.

4.2 Optimal Dosage of Cisplatin to Induce Senescence in Cancer Cell Lines

In order to determine the appropriate dosage of Cisplatin to induce senescence in the different cancer cell lines, WST1 assays were performed. The WST1 assay allowed us to determine the IC50 value of CMT167, LLC, 602, and MOC1 when treated with Cisplatin. From Figure 1, we determined that both MOC1 and CMT167 showed marked resistance to Cisplatin compared to the more sensitive 602 and LLC cell lines. The IC50 values for CMT167 and MOC1 was around 10-20uM, while the IC50 values for 602 and LLC was around 2.5uM.

After further experimentation, it was determined that a cisplatin concentration of 7.5µM for MOC1, 10µM for CMT167, and 2.5µM for both LLC and 602 was optimal to induce senescence without causing a high degree of apoptosis.

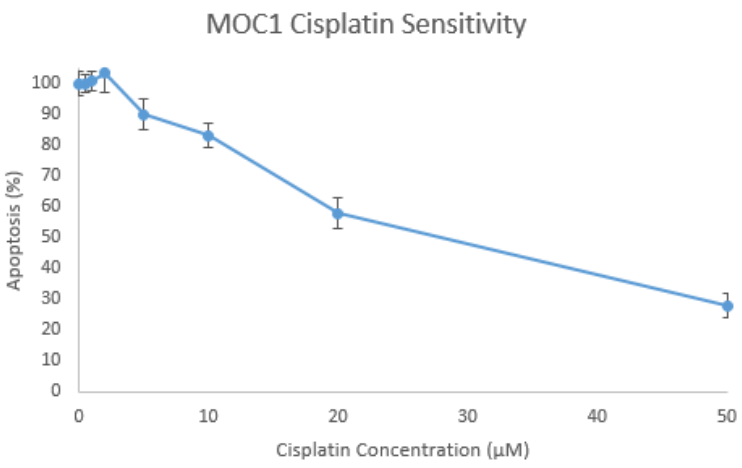

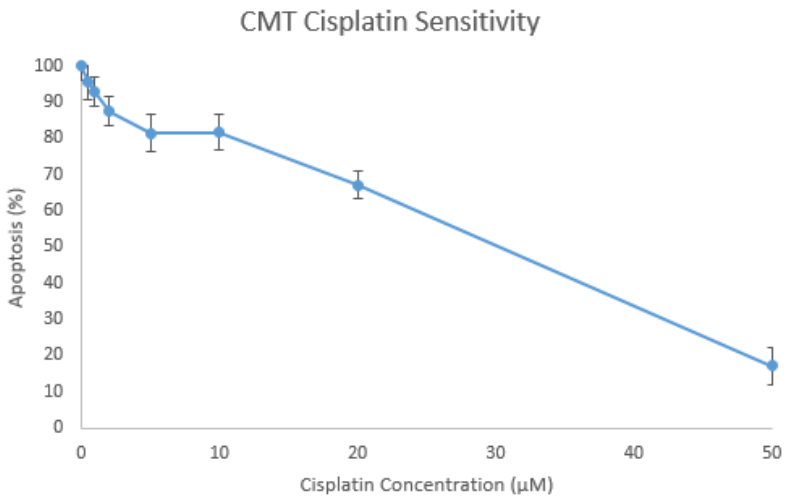

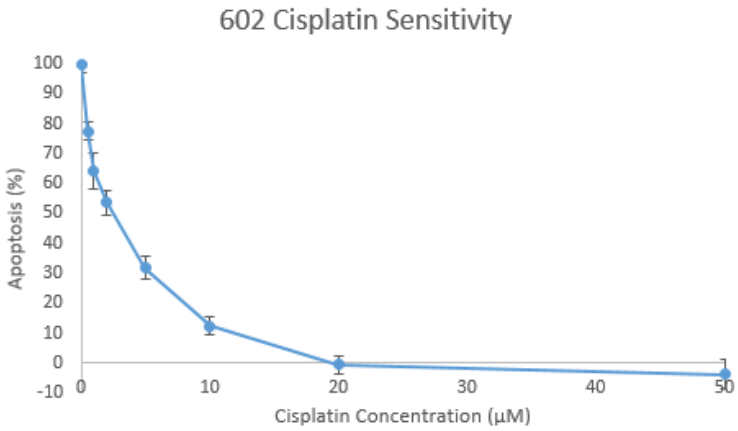

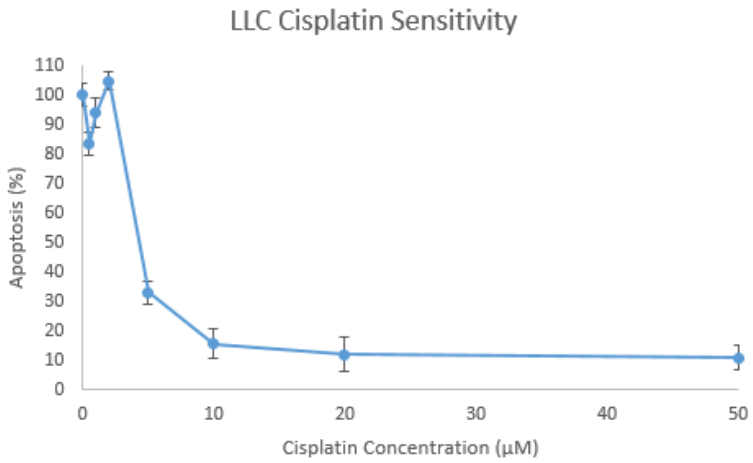

Figure 1: WST1 Cell Proliferation Assays
Each cell line was treated with a cisplatin titration with concentrations 0.5 µM, 1 µM, 2 µM, 5 µM, 10 µM, 20 µM, and 50 µM. After three days a WST1 reagent was added to each well and absorbance was read at 450 nm. MOC1 and CMT were more resistant to cisplatin with 7.5 µM and 10 µM being optimal to induce senescence, respectively. 602 and LLC were more sensitive to cisplatin with 2.5 µM being optimal to induce senescence.

4.3 Cisplatin Does Induce Senescence in Both HNSCC and NSCLC

In order to definitively show that cells were induced into senescence, it was necessary to perform β-Galactosidase staining. It has been shown that cells in senescence have increased lysosomal biogenesis, as well as, heightened expression of the *GLB1* gene, which encodes the lysosomal enzyme β-galactosidase (de Mera-Rodríguez, 2021). When the synthetic substrate X-Gal (5-bromo-4-chloro-3-indoyl-β-d-galactopyranoside) is introduced to senescent cells, its increased cleavage by β-galactosidase produces a blue hue. Figure 2 shows, that all four cell lines were induced into senescence through differential treatment with cisplatin. As expected, a higher rate of LLC and 602 cells stained blue compared with MOC1 and CMT167. This reflects the increased resistance of MOC1 and CMT167 to cisplatin. Approximately 98%±1% of TIS

LLC and 602 cells stained blue when exposed to X-gal, compared to the roughly 45%±4% and 52%±3% of TIS MOC1 and CMT, respectively.

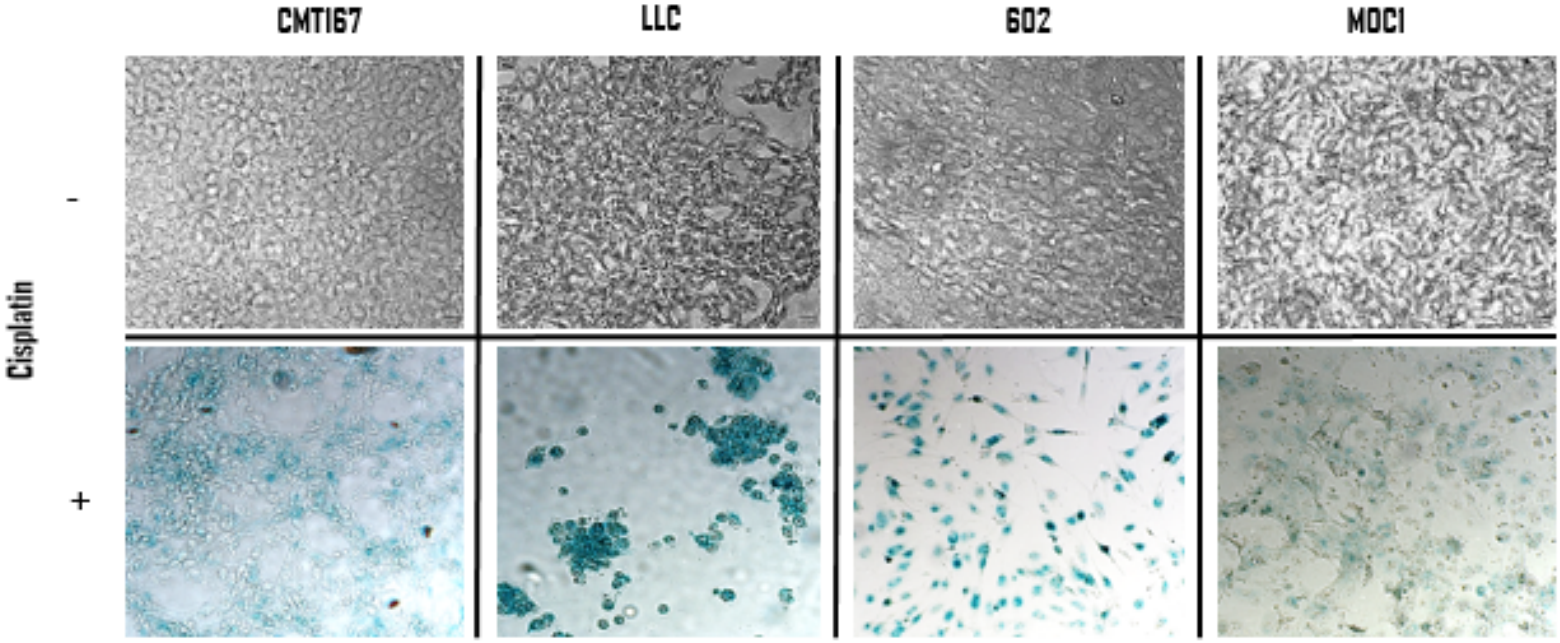

Figure 2: β-galactosidase Staining
Each cell line was first induced into senescence using cisplatin. After five days, the cell lines were stained with the X-gal substrate to determine qualitatively if the cells were in senescence. Approximately 98% of LLC and 602 cell stained blue, while roughly 45% and 52% of MOC1 and CMT cells stained blue, respectively.

4.4 Combination Therapy of Cisplatin Followed by Dual BCL-X_L/BCL-2 Inhibitors, ABT-263 or AZD-4320, Significantly Reduces Viability of HNSCC and NSCLC Cells

Once we had elucidated the cisplatin concentration necessary to induce each individual cell line into senescence, we wanted to test the efficacy of the senolytic agents ABT-199, A-1155463, ABT-263, and AZD-4320. Figure 3 shows comparative Crystal Violet stains of the four different cell lines with cisplatin treatment and without cisplatin treatment. The top row of each cell group is the control group that received no cisplatin treatment. The bottom row of each cell group is the experimental group that received cisplatin treatment to induce the cells into senescence. Each well was treated with either DMSO, or 1 μM of ABT-199, A-1155463, ABT-

263, or AZD-4320. In the control group of CMT167, MOC1, and 602, the senolytic agents had little effect on cell viability compared with DMSO. However, in the experimental group, these cell lines showed more sensitive to the senolytic agents, affirming that there is a synergistic effect between Cisplatin and the senolytic agents. In addition, there is a marked sensitivity to the dual-target inhibitors ABT-263 and AZD-4320 compared to the single-target inhibitors ABT-199 and A-1155463.

In the LLC group, there is little difference between the control group and the experimental group in combination with the four senolytic agents. This is likely due to LLC's inherent sensitivity to inhibition by BH3-mimetics and, as such, induction into senescence is not necessary to sensitize this cell line. In this circumstance, ABT-199, A-1155463, ABT-263, and AZD-4320 are not acting as senolytic agents but as traditional chemotherapies.

When comparing the potency of the individual senolytic agents, the dual, BCL-2 & BCL-X_L, inhibitors ABT-263 and AZD-4320 are superior to the single target inhibitors ABT-199 (BCL-2 inhibitor) and A-1155463 (BCL-X_L inhibitor). This was expected, as many cancer cell lines will upregulate both anti-apoptotic proteins BCL-2 and BCL-X_L in response to cisplatin treatment. Therefore, inhibition of BCL-2 or BCL-X_L alone is not as effective as inhibiting both. Furthermore, when comparing the effectiveness of the single target inhibitors in CMT167, MOC1, and LLC, A-1155463 is more effective than ABT-199. These three cell lines most likely rely more on the anti-apoptotic functions of BCL-X_L compared with BCL-2 This shows that BCL-X_L is the main target for inhibition in these cancer cell lines.

In 602, however, we see that ABT-199 may be comparable to A-1155463 in exerting its cytotoxic effects. This suggests that 602 relies more on the anti-apoptotic functions of BCL-2 compared with the other cell lines, and that both BCL-2 and BCL-X_L should be inhibited when treating this cell line.

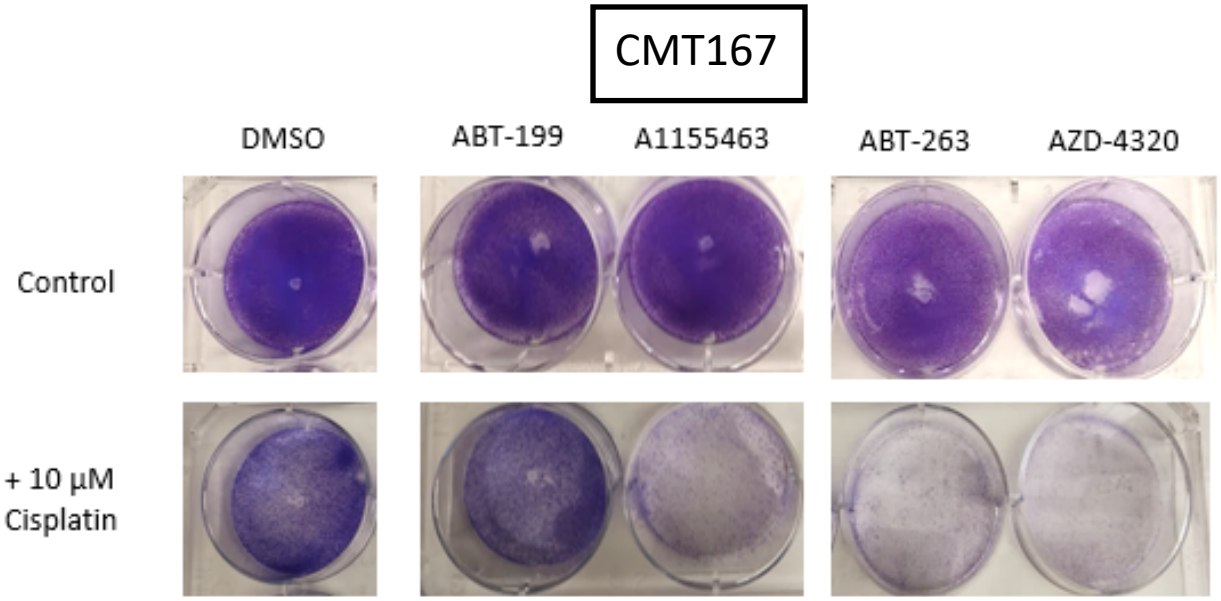

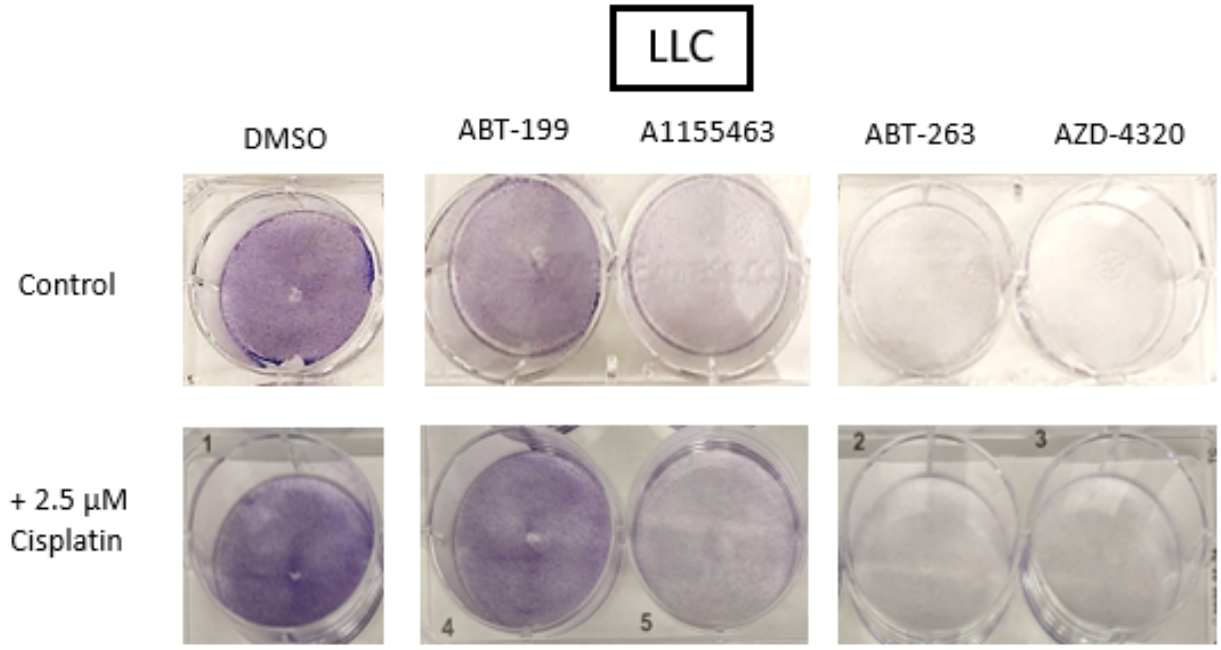

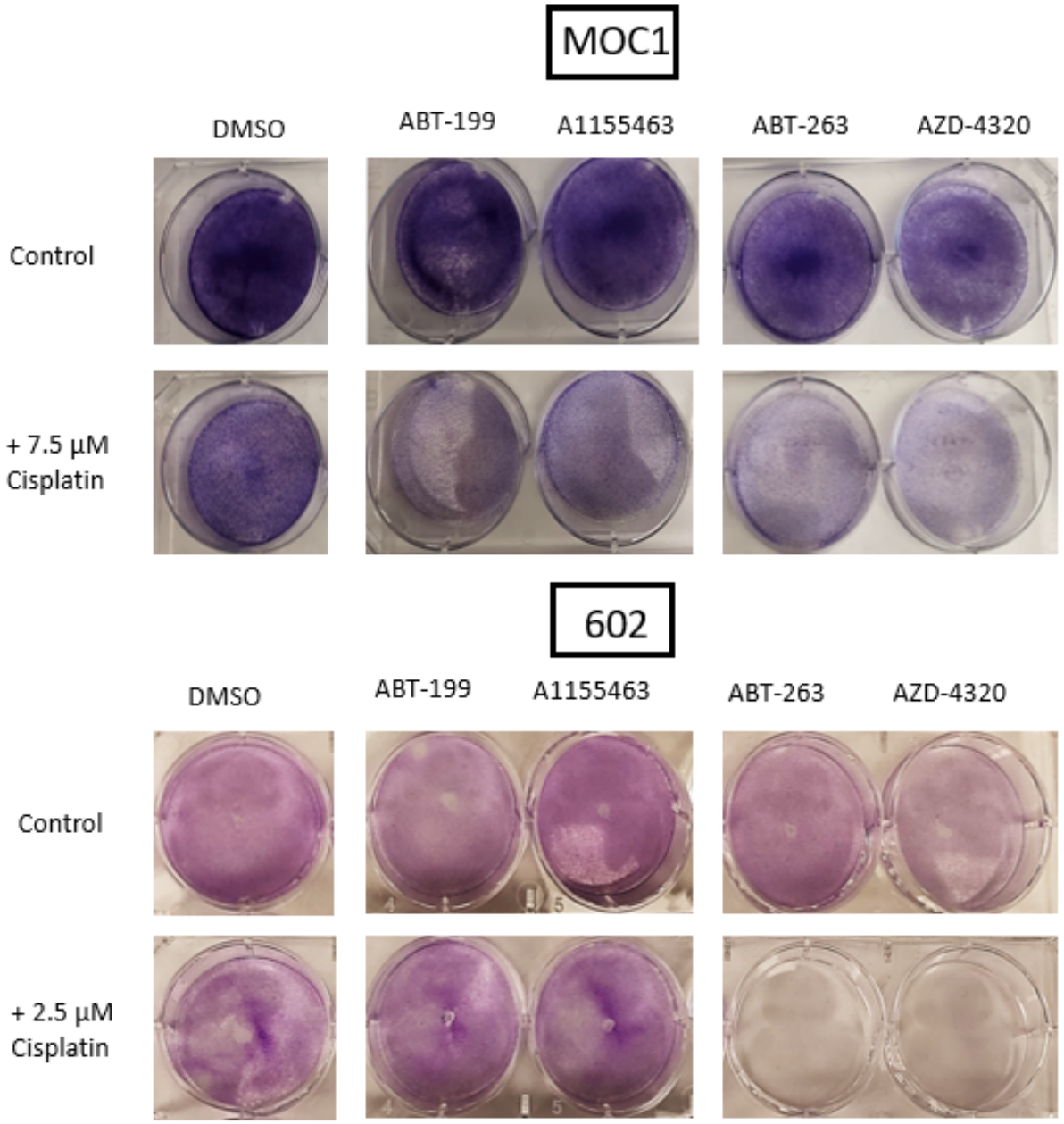

Figure 3: Crystal Violet Staining
Crystal violet staining was used to show cell viability after treatment with cisplatin and various senolytic agents. All wells were treated with 1 µM of senolytic agents. It is clear that the dual BCL-X_L/BCL-2 inhibitors, ABT-263 and AZD-4320, are more potent senolytics than the single target inhibitors A1155463 and ABT-199.

4.5 ABT-263 and AZD-4320 Are Just as Effective as Combinational Treatment with ABT-199 + A-1155463 in MOC1 and 602 Cells

In order to determine the effectiveness of the dual-target inhibitors ABT-263 and AZD-4320, crystal violet staining was performed on both MOC1 and 602. Cisplatin at a concentration of 2.5 µM for 602 and 7.5 µM MOC1 was added to the wells. Four days later senolytics at a concentration of 1 µM were added to the wells. DMSO was used as a control. Crystal violet staining solution (0.05% v/v) was added to the wells on day five. Figure 4 shows that in both cell lines, 1µM of either ABT-263 or AZD-4320 was just as effective as a combination treatment of 1 µM ABT-199 + 1 µM A-1155463.

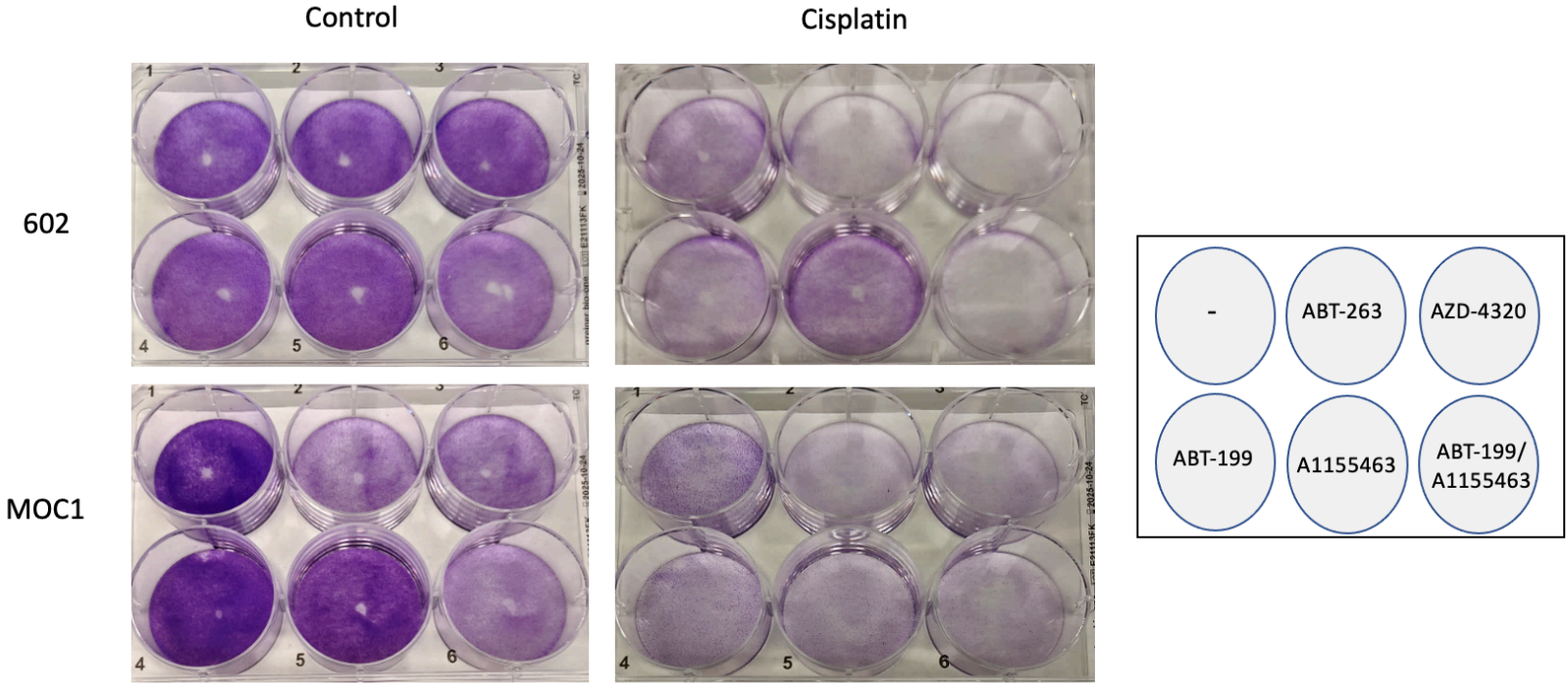

Figure 4: Crystal Violet Staining to Determine Effectiveness of Dual BCL-2/BCL-X_L Inhibitors
Both 602 and MOC1 were treated with 2.5µM and 7.5µM cisplatin. Four days later senolytics were added to both the control and cisplatin treated plates. On day five, plates were stained with 0.05% crystal violet staining solution.

4.6 Cisplatin Increases Gene Expression of the Anti-Apoptotic Proteins BCL-X_L and/or BCL-2 and Combination Cisplatin + AZD-4320 Has a Synergistic Effect

Once it was determined that AZD-4320 is as effective at eradicating TIS cancer cells as ABT-263 in several different cancer cell lines, western blotting was performed to determine the relative expression of key proteins. Cisplatin, a platinum-based DNA damaging agent, induces cells into senescence. In addition, in response to the damage caused by cisplatin treatment, cancer cells are expected to increase the expression of the anti-apoptotic proteins BCL-2 and BCL-X_L.

In Figure 5, we first observed the expression of BCL-2 and BCL-X_L, with and without cisplatin treatment, in both NSCLC cell lines, CMT167 and LLC, and HNSCC cell lines, MOC1 and 602. All cell lines were treated with differing concentrations of cisplatin over a period of 5 days to induce senescence, as confirmed by β-gal staining and morphological changes in the cultured cells. Cells were treated with AZD-4320 (0.2 μM) alone or in combination with cisplatin. After treatment with AZD-4320, cells were harvested 3-4 hours later.

In each cell line, the levels of BAX remained relatively constant with and without treatment. This suggests that BAX expression is not changed with cisplatin or AZD-4320 treatment. Cisplatin induces upregulation of the anti-apoptotic proteins BCL-X_L/BCL-2, while AZD-4320 merely inhibits the interaction of BAX and BCL-X_L/BCL-2 at their BH3 domains. In addition, BAK was not expressed in any cell line at any detectable level. Cleaved caspase-3 is used as a marker for apoptosis, as an increase in cleaved caspase-3 expression is indicative of cell death. Finally, GAPDH is used as a loading control to show that each lane received an equal amount of cell extract.

After treatment with 10 μM cisplatin, CMT167 showed a marked increase in BCL-X_L expression. BCL-2 is expressed at low levels in CMT167 cells with and without cisplatin treatment. This correlates with the crystal violet staining in Figure 3, that shows that A-1155463 (BCL-X_L specific inhibitor) is much more potent than ABT-199 (BCL-2 specific inhibitor). The cisplatin + AZD-4320 combination treatment shows a synergistic effect, with increased levels of cleaved caspase-3, when compared to the AZD-4320 single treatment. This also correlates with Figure 3, as CMT167 cells induced into senescence were much more prone to damage by the senolytic agent AZD-4320, than CMT167 cells not in senescence.

LLC was treated with 2.5 μM cisplatin to induce senescence. As shown in Figure 4, the expression of BCL-X_L remains relatively constant pre- and post-cisplatin treatment, however, there is a slight increase in the level of BCL-2 expression. While LLC does express some basal levels of BCL-2, BCL-X_L is still most likely the main target due to its heightened expression; as well as LLC's increased sensitivity to A-1155463 compared to ABT-199, shown in Figure 3. Of note, AZD-4320 alone can exert its cytotoxic effects in the presence and absence of cisplatin in both NSCLC cell lines (CMT167 and LLC), as depicted by the levels of cleaved caspase-3 expression (Figure 5). This is also consistent with the data from Figure 3, which showed that senescence is not necessary to sensitize CMT167 and LLC to AZD-4320.

602 showed some increase in both BCL-X_L and BCL-2 when treated with 2.5 μM cisplatin. The combination of cisplatin + AZD-4320 also showed a synergistic effect and was much more potent at inducing apoptosis compared to AZD-4320 alone. Of note, 602 seems to rely more on the anti-apoptotic functions of BCL-2 compared to BCL-X_L. This is suggested by the increased expression of BCL-2 with cisplatin treatment in Figure 5, as well as the increased sensitivity to ABT-199 over A-1155463 in Figure 3.

MOC1 was treated with 7.5 µM cisplatin and showed a marked increase in BCL-X_L expression. Furthermore, the combination of cisplatin+AZD-4320 showed a dramatic increase in cleaved caspase-3 compared to AZD-4320 alone. MOC1 expresses minimal levels of BCL-2 even when induced into senescence and validates the results from Figure 3, as MOC1 was much more sensitive to A-1155463 compared to ABT-199.

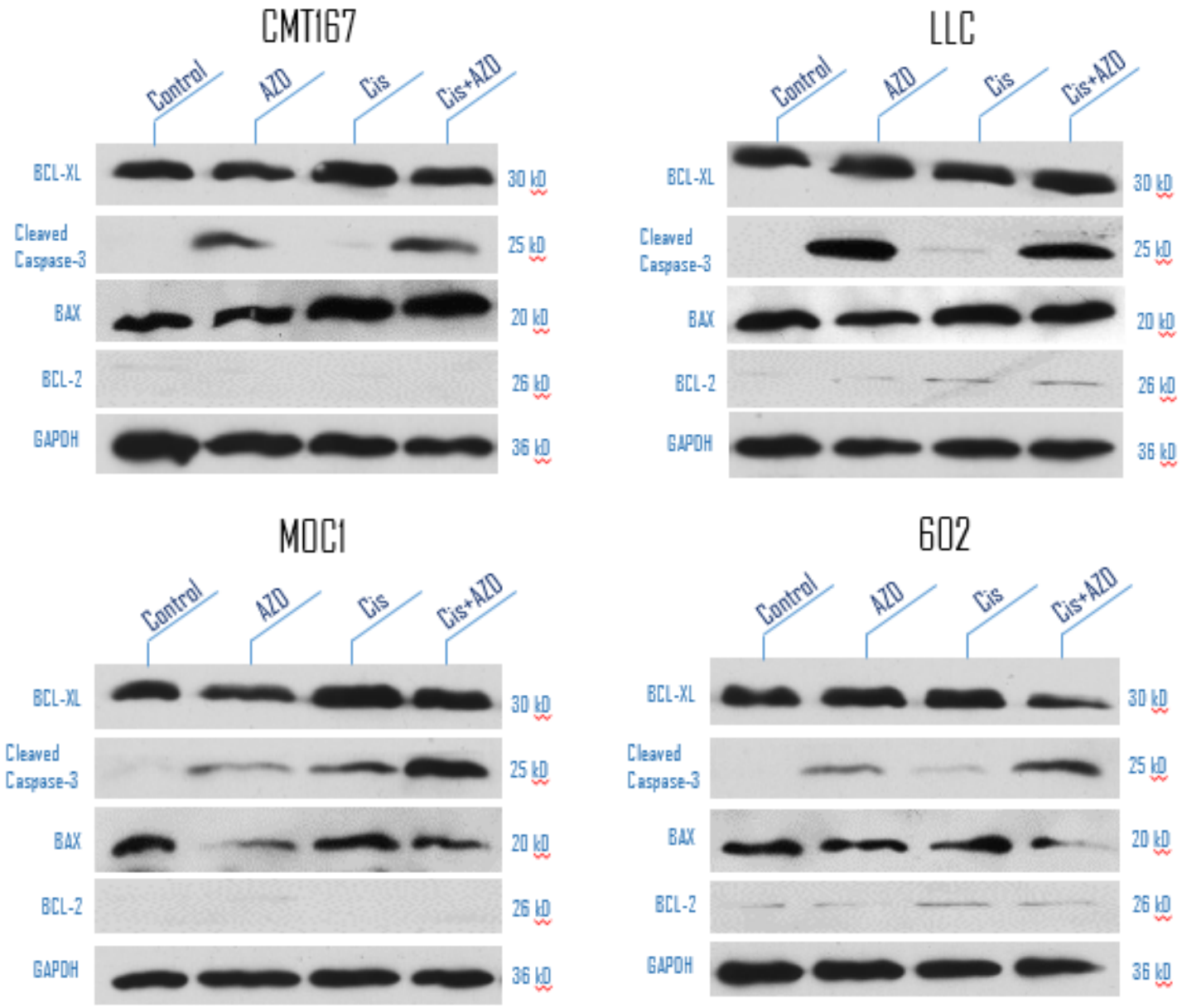

Figure 5: Western Blot Analysis
Western blot analysis was performed after treatment with 0.2 µM AZD-4320, cisplatin, and a combination of cisplatin+AZD-4320. Caspase-3 was used as a marker for apoptosis and GAPDH was used as a loading control. Cells were harvested 5 days post-cisplatin treatment.

4.7 Observing Cell Viability with Cisplatin and Combination Treatment Using Florescence Activated Cell Sorting (FACS)

To further confirm the results from Figure 5, FACS analysis was performed on MOC1 to determine the relative viability of MOC1 cells with both single and combination treatment. As expected, the AZD-4320 or cisplatin treatment group showed some level of cell death. However, the combination therapy showed a slightly greater effect than between both AZD-4320 and cisplatin alone. In Figure 5, we see a higher degree of cleaved caspase-3 expression in the cisplatin treated group relative to the AZD-4320 treated group. In addition, in Figure 6, we see an increase in apoptosis in the cisplatin treatment group compared to the AZD-4320 treatment group. This is because cisplatin alone is a highly toxic chemotherapeutic agent, especially to the rapidly dividing HNSCC cells. Furthermore, the basal level of BCL-X_L is relatively low in the AZD-4320 treatment group. When the cells are treated with cisplatin, however, we see increased expression of BCL-X_L. The combination of cisplatin and AZD-4320 causes an increase in the expression of BCL-X_L allowing for more inhibition by AZD-4320 and subsequently more cell death.

No statistically significant difference between cisplatin and cisplatin + AZD-0466 was observed in Figure 6 ($p=.1766$). This may be due to the length of time the cells were exposed to cisplatin treatment. If cells are exposed to cisplatin for too long a period of time they will begin to undergo apoptosis due to the high toxicity of cisplatin. This data represents an additive effect of cisplatin in combination with AZD-4320 rather than a synergistic effect.

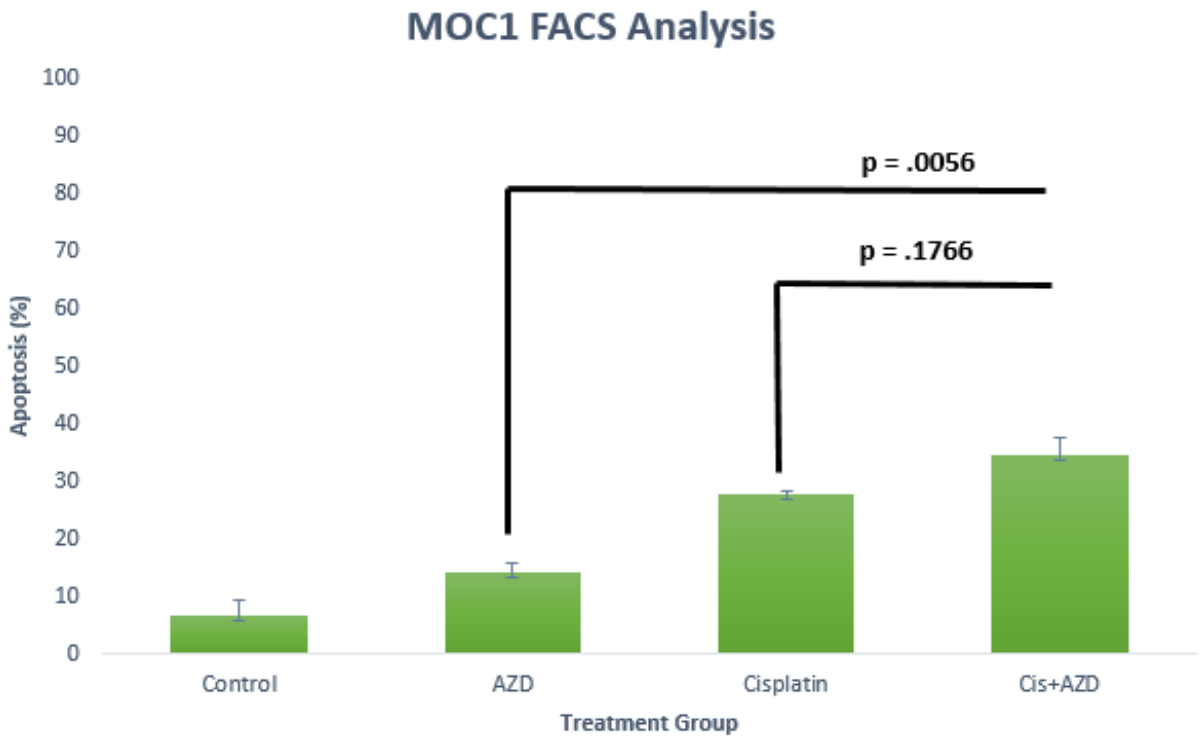

Figure 6: Fluorescence Activated Cell Sorting Analysis of MOC1
FACS analysis was used to determine the viability of MOC1 cells after treatment with 0.2 µM AZD-4320, 7.5 µM cisplatin, and a combination of cisplatin + AZD-4320. Annexin-V and Propidium Iodide were used as indicators to determine the relative amount of apoptosis occurring within each treatment group.

4.8 Determining the Effectiveness of Cisplatin + AZD-0466 Combination Treatment in a MOC1 Mouse Xenograft Model

Due to the dramatic increase in BCL-X_L, and high apoptosis rate in the cisplatin + AZD-4320 combination treatment, shown in Figure 5, MOC1 was chosen for a pilot study in mouse xenograft models. The pilot study was used to determine if the results from the *in vitro* study would transfer to a live animal model. C57BL/6, immune competent, female mice were injected with $1x10^5$ MOC1 cells orthotopically on the left cheek. It is important to note that MOC1 cells are established from the same strain of C57BL/6 mice, therefore, the MOC1 cells were not

rejected by the mouse's immune system. The MOC1 cells were previously transfected with the luciferase gene. This allowed for fluorescent imaging of orthotopic tumor growth when the luciferin substrate was introduced subcutaneously in mice.

A drug-dendrimer conjugate of AZD-4320, AZD-0466, was used in place of AZD-4320 for *in vivo* studies. AZD-4320 was not tolerated well in live animal models as it was shown to have low solubility in addition to cardiovascular toxicity. Dendrimers are branched polymers that are built up of highly concentric monomers, making them highly soluble in water. AZD-0466 is composed of the AZD-4320 molecules that are been chemically conjugated to free lysines on a poly-L-lysine dendrimer. This drug-dendrimer conjugate of AZD-4320 showed increase exchange between plasma and tumor cells, with increased cardiovascular tolerance. (Patterson, 2021).

Twenty C57BL/6 mice were divided into four separate treatment groups: control, cisplatin treated, AZD-0466, and a combination of cisplatin and AZD-0466 treated. One-week post-MOC1 inoculation, tumors were palpable and the mice were randomized into the four treatment groups (n = 5) based on tumor size. Cisplatin and/or AZD-0466 treatment began one-week post-MOC1 inoculation. Cisplatin (5 mg/kg) was administered intraperitoneally once a week for two weeks to induce the tumor cells into senescence. AZD-0466 (100 mg/kg) was administered by tail vein injection once a week for two weeks.

Once the MOC1 tumors had grown to be palpable on the left cheek, IVIS (*in vivo* Imaging Systems) and digital caliper measurements were used to track disease progression twice a week.

Figure 7 and 8 show disease progression through both digital caliper measurements and IVIS, respectively. One mouse from both the cisplatin and AZD-0466 treatment group developed ulcerated tumors and had to be euthanized midway through the study. It is clear from the data that there is a synergistic effect between cisplatin and AZD-0466. Tumor volume was significantly reduced in mice that received simultaneous treatment with cisplatin and AZD-0466 compared to either treatment alone. In addition, we observed that each single treatment does have a therapeutic effect when compared with the control group. This *in vivo* study validates the results from Figure 4, which shows some apoptosis in single treatment groups and a dramatic increase in apoptosis with combination therapy.

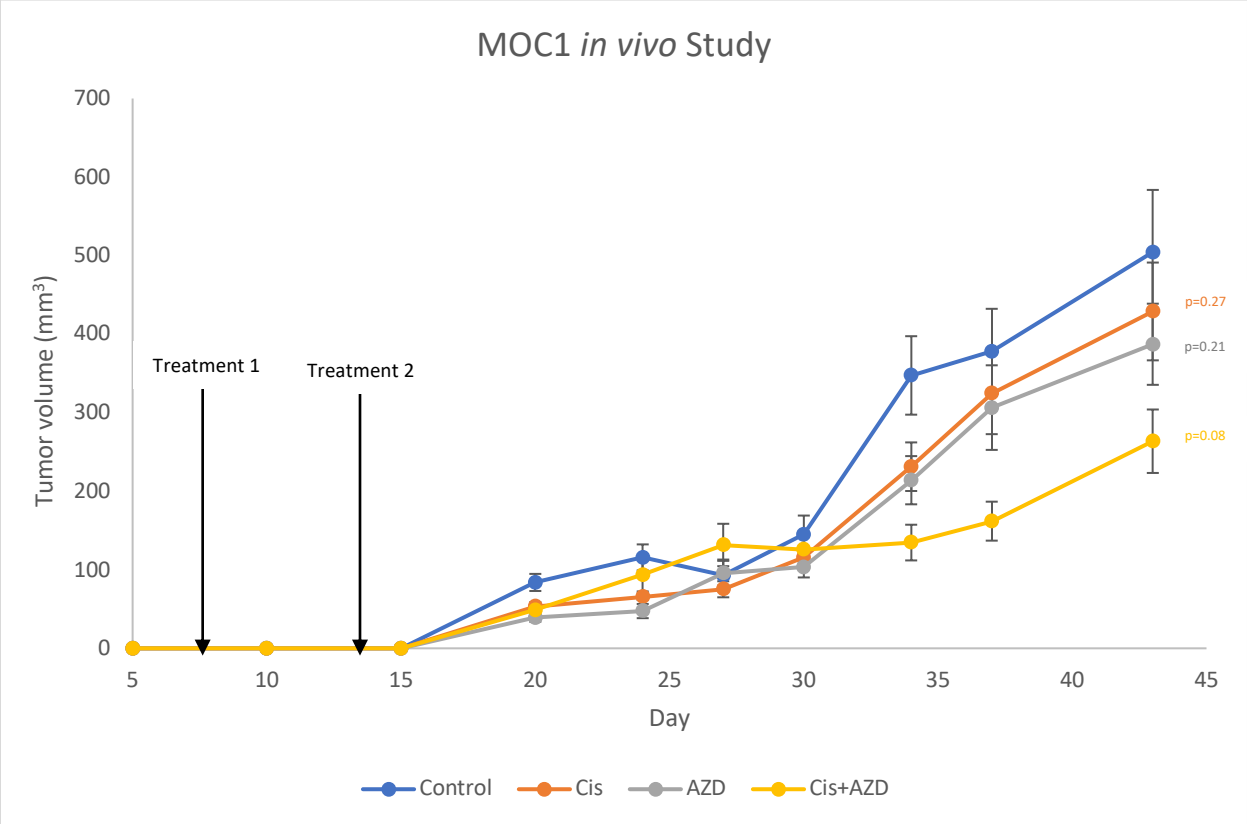

Figure 7: MOC1 Mouse Xenograft Study using C57BL/6 Mice
C57BL/6 mice were inoculated with $1x10^5$ MOC1 cells in the left cheek. Once tumors were palpable, the mice were randomized into four groups: control, cisplatin, AZD-0466, and cisplatin+AZD-0466. Mice were treated with cisplatin (5 mg/kg) intraperitoneally once a week for two weeks. AZD-0466 (100 mg/kg) was administered by tail vein injection once a week for two weeks.

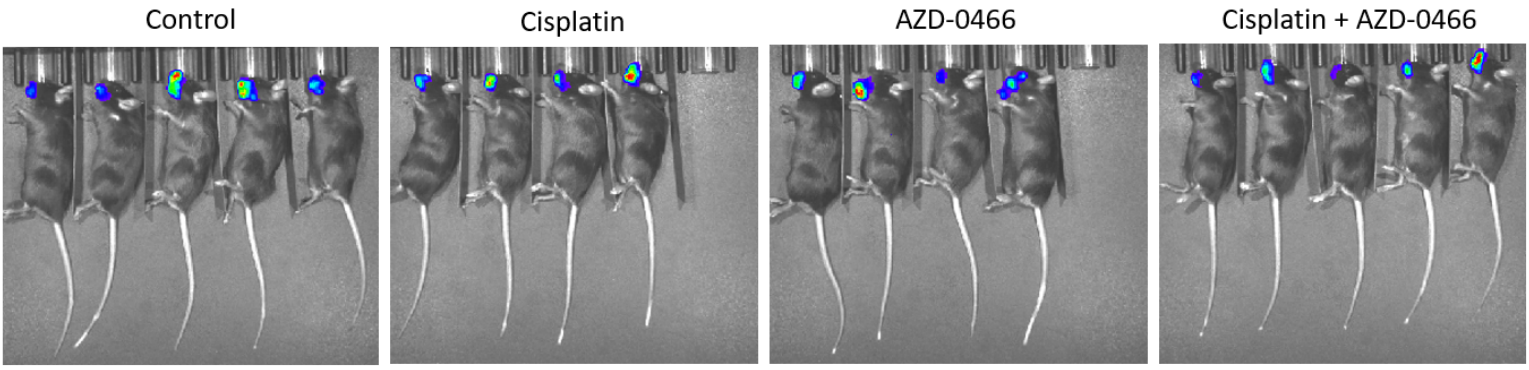

Figure 8: MOC1 C57BL/6 Mouse IVIS imaging
MOC1 cells were previously transfected with the luciferase gene. C57BL/6 mice were treated with the luciferin substrate once a week to track disease progression using IVIS imaging. The amount of light produced, flux, is directly proportion to the growth of the tumors for each treatment group. One mouse from both the cisplatin and AZD-0466 treatment group developed ulcerated tumors and had to be euthanized midway through the study.

4.9 Pilot Study to Determine if CMT or LLC is a Better Candidate for NSCLC Mouse Xenograft Model

After successful completion of the HNSCC *in vivo* study, we needed to determine the efficacy of AZD-0466 in a NSCLC mouse model. First, we carried out a pilot experiment to determine which NSCLC cell line responded better to cisplatin treatment *in vivo*.

A total of sixteen male C57BL/6 were used for this study. Eight mice were inoculated with 1 x 10^6 LLC cells and eight mice were inoculated with 1 x 10^6 CMT167 cells at the left flank. One-week post-inoculation the mice were randomized into two different treatment groups, four control mice and four cisplatin treated mice for both the LLC and CMT167 models. Cisplatin (5mg/kg) treatment began one-week post-inoculation and was administered intraperitoneally once a week for two weeks to induce the cells into senescence.

Tumors were measured with a digital caliper once they had emerged from the left flank and were palpable. It is important to note that neither LLC or CMT167 cells were previously transfected with the luciferase gene, and as such IVIS imaging was not possible.

As can be seen in Figure 9, the LLC tumors progressed much more rapidly than the CMT167 tumors. All four LLC control mice were sacrificed 17 days into the study as their tumors were at the humane endpoint of 2,000 mm^3. Conversely, the CMT167 control mice survived up until the end of the study at around day 24, and the average tumor size was still under 2,000 mm^3. Cisplatin treatment had a significant effect on the LLC mice compared with the LLC control group. The cisplatin treated mice survived until the end of the study and showed an average tumor size of less than half of the LLC control mice. Conversely, cisplatin treatment had a minimal effect on the CMT167 mice and there was no significant difference in tumor size between the CM167T cisplatin treated group and the CMT167 control group. This correlates with the increased resistance of CMT167 to cisplatin treatment as determined in Figure 1. Based on the results from Figure 9, it was decided that LLC would be used as the NSCLC *in vivo* model.

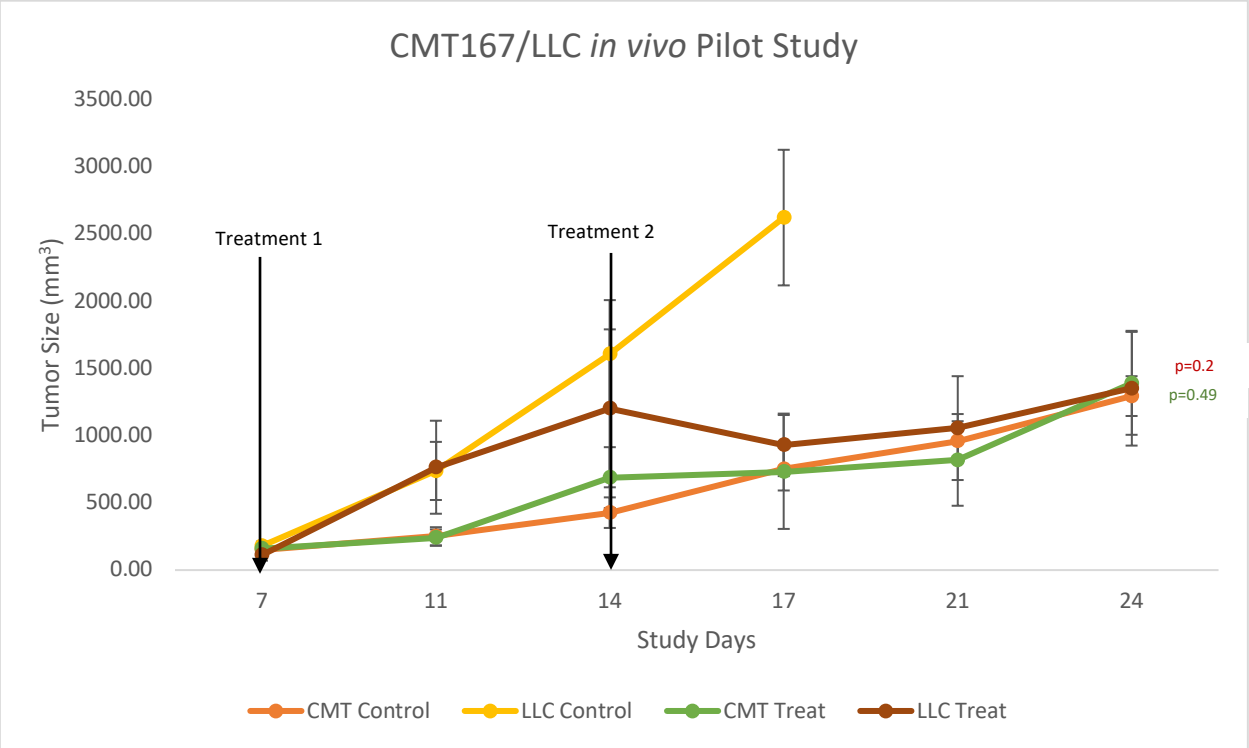

Figure 9: CMT167/LLC Mouse Xenograft Pilot Study Using C57BL/6 Mice
C57BL/6 mice were inoculated with $1x10^6$ CMT or LLC cells on the left rear flank. Once tumors were palpable, the mice were randomized into two groups (n=4) for each cell line control and cisplatin treated. Cisplatin (5 mg/kg) was administered intraperitoneally once a week for two weeks.

4.10 Determining the Senolytic Capabilities of AZD-0466 in an LLC Mouse Xenograft Model

Once LLC was identified as our *in vivo* NSCLC model, we wanted to determine the senolytic capabilities of AZD-0466. Twenty male C57BL/6 mice were inoculated with $1x10^6$ LLC cells at their left flank. One-week post inoculation, LLC tumors were palpable and the mice were randomized into four groups based on tumor size: control, AZD-0466 treated, cisplatin treated, and a combination of cisplatin + AZD-0466 treated. Cisplatin (5 mg/kg) treatment began one-week post-inoculation and was administered intraperitoneally for two weeks to induce senescence. AZD-0466 100 mg/kg was administered by tail vein injection once a week for two weeks.

Figure 10 shows the results of the LLC *in vivo* study. It is clear that cisplatin alone is effective against LLC cells which correlates with the cisplatin sensitivity displayed in Figure 1. There are some discrepancies between the results of the LLC *in vivo* study and the CMT167/LLC *in vivo* pilot study. First, while the LLC control group in Figure 10 did show increased tumor proliferation compared to all three treatment groups, the mice survived more than twice as long as they did in the pilot study (Figure 9). This may be due to an increased immune response in the LLC mice for the LLC *in vivo* study compared with the CMT167/LLC *in vivo* pilot study. The role of the immune system in cancer progression is currently being researched, and it may be that the LLC mice in Figure 9 evoked a weaker immune response than the LLC mice in Figure 10. This could result in faster, more aggressive tumor proliferation. Another discrepancy that needs to be addressed is the sensitivity to cisplatin vs. AZD-0466, when comparing the *in vivo* results from Figure 10 and the western blot results from Figure 5. The *in vivo* study showed a significant sensitivity to cisplatin compared to the sensitivity depicted by cleaved caspase 3 expression in Figure 5. Additionally, while AZD-0466 (AZD-

4320+dendrimer conjugate) treatment alone did show some cytotoxic effects in the *in vivo* study, AZD-4320 alone appeared to be much more cytotoxic *in vitro* as shown in Figure 5.

As previously mentioned, when comparing the effects of AZD-4320 treatment alone *in vitro* in NSCLC vs. HNSCC, it is clear that NSCLC is much more sensitive to AZD-4320 in a non-senescent state. This can be seen in the decreased viability of CMT167 and LLC in Figure 3, and by the increased cleaved caspase 3 expression of CMT167 and LLC in Figure 5, with AZD-4320 treatment alone. Alternatively, the HNSCC cell lines, MOC1 and 602, are much more prone to damage by AZD-4320 *in vitro* when first induced into senescence by cisplatin, compared to AZD-4320 treatment alone.

There are several reasons that may explain the decreased effect of AZD-0466 *in vivo* vs. AZD-4320 *in vitro*, in the LLC cell line. First, AZD-4320 alone could not be advanced to clinical trials due to its low-solubility (highly hydrophobic) and high degree of plasma protein binding. This necessitated the formulation of the drug-dendrimer conjugate AZD-0466 in order to reduce cardiovascular toxicity and enhance plasma to tumor transition of AZD-4320 (Patterson, 2021). It is likely that AZD-4320 *in vitro* is more potent than AZD-0466 *in vivo* because AZD-4320 is more readily accessible to LLC cells in culture compared to AZD-0466 in a live animal model. AZD-0466 must travel through the bloodstream and then transition from the plasma into tumor cells at the left flank of the mouse, while AZD-4320 can directly pass through the cell membrane of LLC cells in culture.

Another potential explanation for the decreased effect of AZD-0466 *in vivo* compared to AZD-4320 *in vitro* is presence and absence of the immune system, respectively. The C57BL/6 mice are immune competent and therefore the actions of their immune system cannot be overlooked. It is likely that upon inoculation with LLC cells, the mouse's innate immune system

was recruited to the site of the tumor, and potentially slowed down tumor progression. The innate immune system consists of phagocytes (neutrophils, monocytes, and macrophages) along with NK cells. Previously research has shown that genetic alterations in cancer cells can pre-dispose them to complement-mediated cell death. However, as the tumors continue to grow, they are able to evade immune surveillance by altering their gene expression and cell surface proteins (Pandya, 2016). Thus, while mounting an initial immune response may decrease tumor progression at the beginning, ultimately cancer cells are able to manipulate the immune system into TME that allows for the continued proliferation and expansion of cancer cells.

In Figure 10, we see that cisplatin most likely induces senescence as tumor size is consistently slow to increase throughout the entirety of the study. However, in the AZD-0466 treatment group we began to see a gradual increase in tumor size around day 19. This may be the point at which the mouse's immune response has been attenuated. Furthermore, after day 23 all mice in the AZD-0466 treatment had to be euthanized due to increased tumor volume reaching the humane endpoint. The presence of the immune system may account for the discrepancies between AZD-0466 treatment alone *in vivo* and AZD-4320 treatment alone *in vitro*.

LLC may respond equally to cisplatin treatment alone and combination of cisplatin + AZD-0466 as depicted by the results in Figure 10. However, the potential for cancer re-emergence from the TIS state should not be overlooked. While cisplatin at lower concentrations may induce senescence alone, cisplatin + AZD-0466 allows complete eradication of the senescent cells.

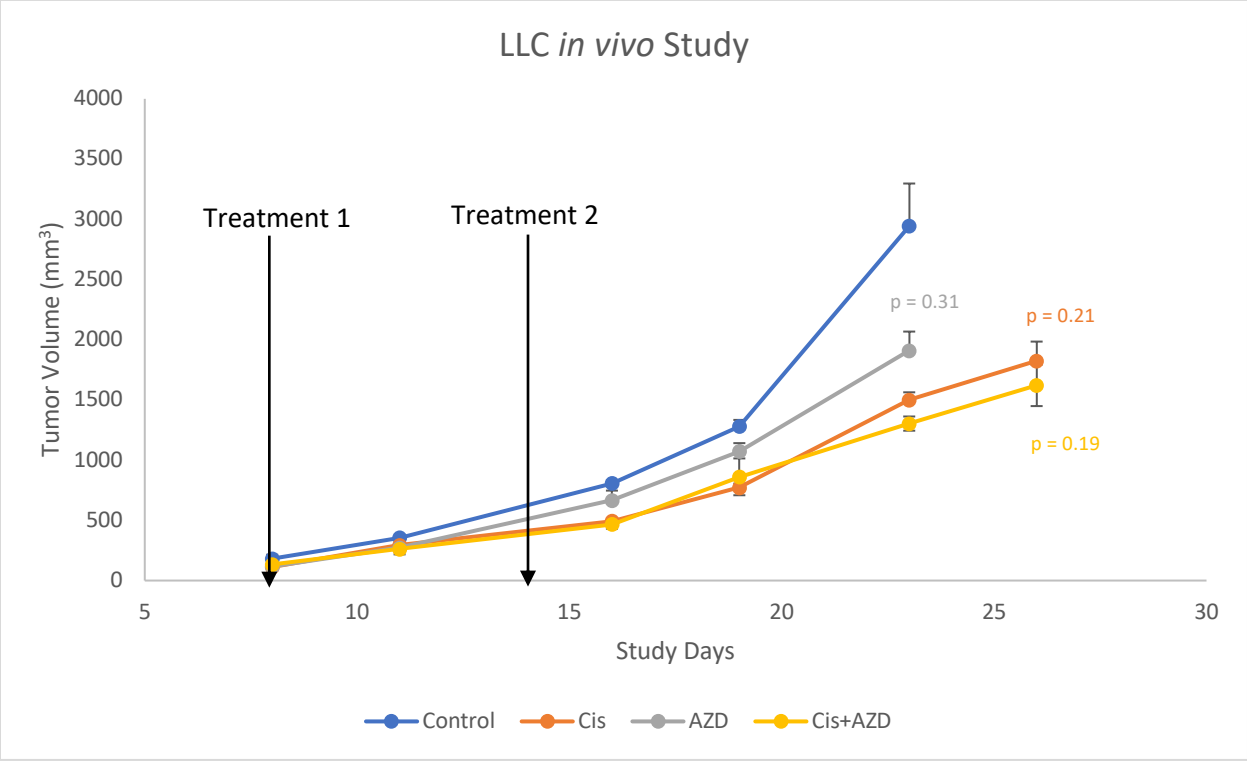

Figure 10: LLC Mouse Xenograft Study Using C57BL Mice
C57BL/6 mice were inoculated with $1x10^6$ LLC cells in the left rear flank. Once tumors were palpable the mice were randomized into four groups (n=5): control, cisplatin, AZD-0466, and cisplatin + AZD-0466. Cisplatin (5 mg/kg) was administered intraperitoneally once a week for two weeks. AZD-0466 100 mg/kg was administered by tail vein injection once a week for two weeks.

Conclusion:

Both ABT-263 and AZD-4320 are potent senolytics in several cell lines. Their mode of action is through the dual inhibition of the anti-apoptotic proteins BCL-2 and BCL-X_L. This was shown in three different cell lines from two different types of cancer. Once induced into senescence using the DNA-damaging agent cisplatin, the HNSCC cell lines MOC1 and 602 displayed marked sensitivity to the senolytic agents ABT-263 and AZD-4320. The NSCLC cell line CMT167 showed similar results as TIS sensitized these cells to the senolytics ABT-263 and AZD-4320 compared with senolytic treatment of non-senescent CMT167 cells. The NSCLC cell line LLC, however, showed somewhat contradictive results when comparing *in vivo* and *in vitro* models. In the *in vitro* models, AZD-4320 alone was enough to induce apoptosis without first inducing the cells into senescence. In this way, AZD-4320 is not working as a senolytic but rather as a traditional cytotoxic drug. However, the *in vivo* model shows that LLC has lower sensitivity to the AZD-4320-dendrimer conjugate (AZD-4066) alone, and has high sensitivity to cisplatin treatment alone. Additionally, there may be a slight synergistic effect between the cisplatin-AZD-0466 combination. Therefore, *in vitro* AZD-4320 may be acting more as a chemotherapy, while *in vivo* it may be acting more as a senolytic.

There may be several factors that account for this discrepancy. First, AZD-4320 may be more readily accessible to its anti-apoptotic targets *in vitro*, as it must simply cross the plasma membrane into the LLC cells. In the *in vivo* model, however, AZD-4320 is quite hydrophobic and therefore must be ligated to a poly-L-lysine dendrimer to increase its solubility in the plasma. In this way, AZD-4320 may not be transitioning into LLC cells at the same rate as it does *in vitro*. Additionally, the C57BL/6 mice are immune competent and inoculation with the

foreign LLC cells may cause an initial, localized innate immune response that decreases tumor progression for a time, before the tumor adapts and produces TME.

Compared with treatment of the single-target inhibitors A-1155463 and ABT-199, it is clear that the dual-target inhibitors ABT-263 and AZD-4320 are more potent senolytics. Furthermore, comparison between A-1155463 (BCL-X_L specific inhibitor) and ABT-199 (BCL-2 specific inhibitor) shows that BCL-X_L is the primary target for inhibition for most TIS cell lines in this study. The HNSCC cell line 602 did show equal sensitivity to both A-1155463 and ABT-199 in the crystal violet staining and showed increased expression of BCL-2 when treated with cisplatin over BCL-X_L in the western blot analysis. This suggests that 602 alone relies on the anti-apoptotic capabilities of both BCL-2 and BCL-X_L.

Future studies should focus on conducting *in vivo* studies of both CMT and 602 to determine the senolytic capabilities of AZD-0466 in immune competent mice. Since AZD-0466 is the clinically relevant form of AZD-4320 it is important to determine its accessibility to tumor cells *in vivo* and also to determine if it is acting as a senolytic or a traditional cytotoxic drug. In addition, studies conducted in immune compromised mice may elucidate some, if any, of the effects that the immune system has on cancer therapies.

Based on the findings from this study, it is clear that cisplatin in combination with AZD-4320 may improve patient outcomes in HNSCC. In NSCLC, cisplatin in combination with AZD-4320 may benefit patient outcomes, however, further studies are warranted.

References

Ahmadinejad F, Bos T, Hu B, Britt E, Koblinski J, Souers AJ, Leverson JD, Faber AC, Gewirtz DA, Harada H. Senolytic-Mediated Elimination of Head and Neck Tumor Cells Induced Into Senescence by Cisplatin. Mol Pharmacol. 2022 Mar;101(3):168-180. doi: 10.1124/molpharm.121.000354. Epub 2021 Dec 14. PMID: 34907000; PMCID: PMC8969145.

Chial, H. (2008) Proto-oncogenes to oncogenes to cancer. *Nature Education* 1(1):33

Cooper GM. The Cell: A Molecular Approach. 2nd edition. Sunderland (MA): Sinauer Associates; 2000. The Development and Causes of Cancer. Available from: https://www.ncbi.nlm.nih.gov/books/NBK9963/

Cornet I, Gheit T, Franceschi S, Vignat J, Burk RD, Sylla BS, Tommasino M, Clifford GM; IARC HPV Variant Study Group. Human papillomavirus type 16 genetic variants: phylogeny and classification based on E6 and LCR. J Virol. 2012 Jun;86(12):6855-61. doi: 10.1128/JVI.00483-12. Epub 2012 Apr 4. PMID: 22491459; PMCID: PMC3393538.

de Mera-Rodríguez JA, Álvarez-Hernán G, Gañán Y, Martín-Partido G, Rodríguez-León J, Francisco-Morcillo J. Is Senescence-Associated β-Galactosidase a Reliable *in vivo* Marker of Cellular Senescence During Embryonic Development? Front Cell Dev Biol. 2021 Jan 28;9:623175. doi: 10.3389/fcell.2021.623175. PMID: 33585480; PMCID: PMC7876289.

Elmore S. Apoptosis: a review of programmed cell death. Toxicol Pathol. 2007 Jun;35(4):495-516. doi: 10.1080/01926230701320337. PMID: 17562483; PMCID: PMC2117903.

Ewald JA, Desotelle JA, Wilding G, Jarrard DF. Therapy-induced senescence in cancer. J Natl Cancer Inst. 2010 Oct 20;102(20):1536-46. doi: 10.1093/jnci/djq364. Epub 2010 Sep 21. PMID: 20858887; PMCID: PMC2957429.

Florea AM, Büsselberg D. Cisplatin as an anti-tumor drug: cellular mechanisms of activity, drug resistance and induced side effects. Cancers (Basel). 2011 Mar 15;3(1):1351-71. doi: 10.3390/cancers3011351. PMID: 24212665; PMCID: PMC3756417

Georges P, Rajagopalan K, Leon C, Singh P, Ahmad N, Nader K, Kubicek GJ. Chemotherapy advances in locally advanced head and neck cancer. World J Clin Oncol. 2014 Dec 10;5(5):966-72. doi: 10.5306/wjco.v5.i5.966. PMID: 25493232; PMCID: PMC4259956

Gibbons DL, Byers LA, Kurie JM. Smoking, p53 mutation, and lung cancer. Mol Cancer Res. 2014 Jan;12(1):3-13. doi: 10.1158/1541-7786.MCR-13-0539. PMID: 24442106; PMCID: PMC3925633.

Hung RJ, McKay JD, Gaborieau V, Boffetta P, Hashibe M, Zaridze D, Mukeria A, Szeszenia-Dabrowska N, Lissowska J, Rudnai P, Fabianova E, Mates D, Bencko V, Foretova L, Janout V, Chen C, Goodman G, Field JK, Liloglou T, Xinarianos G, Cassidy A, McLaughlin J, Liu G, Narod S, Krokan HE, Skorpen F, Elvestad MB, Hveem K, Vatten L, Linseisen J, Clavel-Chapelon F, Vineis P, Bueno-de-Mesquita HB, Lund E, Martinez C, Bingham S, Rasmuson T, Hainaut P, Riboli E, Ahrens W, Benhamou S, Lagiou P, Trichopoulos D, Holcátová I, Merletti F, Kjaerheim K, Agudo A, Macfarlane G, Talamini R, Simonato L, Lowry R, Conway DI, Znaor A, Healy C, Zelenika D, Boland A, Delepine M, Foglio M, Lechner D, Matsuda F, Blanche H, Gut I, Heath S, Lathrop M, Brennan P. A susceptibility locus for lung cancer maps to nicotinic acetylcholine receptor subunit genes on 15q25. Nature. 2008 Apr 3;452(7187):633-7. doi: 10.1038/nature06885. PMID: 18385738.

Johnson DE, Burtness B, Leemans CR, Lui VWY, Bauman JE, Grandis JR. Head and neck squamous cell carcinoma. Nat Rev Dis Primers. 2020 Nov 26;6(1):92. doi: 10.1038/s41572-020- 00224-3. PMID: 33243986; PMCID: PMC7944998.

Kale, J., Osterlund, E. & Andrews, D. BCL-2 family proteins: changing partners in the dance towards death. *Cell Death Differ* **25**, 65–80 (2018). https://doi.org/10.1038/cdd.2017.186

Koontongkaew S. The tumor microenvironment contribution to development, growth, invasion and metastasis of head and neck squamous cell carcinomas. J Cancer. 2013;4(1):66-83. doi: 10.7150/jca.5112. Epub 2013 Jan 1. PMID: 23386906; PMCID: PMC3564248.

Le X, Hanna EY. Optimal regimen of cisplatin in squamous cell carcinoma of head and neck yet to be determined. Ann Transl Med. 2018 Jun;6(11):229. doi: 10.21037/atm.2018.05.10. PMID: 30023392; PMCID: PMC6036002.

Li C, Wang C, Yu J, Fan Y, Liu D, Zhou W, Shi T. Residential Radon and Histological Types of Lung Cancer: A Meta-Analysis of Case–Control Studies. Int J Environ Res Public Health. 2020 Feb 24;17(4):1457. doi: 10.3390/ijerph17041457. PMID: 32102460; PMCID: PMC7068370.

National Institutes of Health (US); Biological Sciences Curriculum Study. NIH Curriculum Supplement Series [Internet]. Bethesda (MD): National Institutes of Health (US); 2007. Understanding Cancer. Available from: https://www.ncbi.nlm.nih.gov/books/NBK20362/

Patterson, C.M., Balachander, S.B., Grant, I. *et al.* Design and optimisation of dendrimer-conjugated Bcl-2/x_L inhibitor, AZD0466, with improved therapeutic index for cancer therapy. *Commun Biol* **4**, 112 (2021). https://doi.org/10.1038/s42003-020-01631-8

Pawlikowski JS, Adams PD, Nelson DM. Senescence at a glance. J Cell Sci. 2013 Sep 15;126(Pt 18):4061-7. doi: 10.1242/jcs.109728. Epub 2013 Aug 22. PMID: 23970414; PMCID: PMC3772382.

Pandya PH, Murray ME, Pollok KE, Renbarger JL. The Immune System in Cancer Pathogenesis: Potential Therapeutic Approaches. J Immunol Res. 2016;2016:4273943. doi: 10.1155/2016/4273943. Epub 2016 Dec 26. PMID: 28116316; PMCID: PMC5220497.

Reyes-Gibby CC, Anderson KO, Merriman KW, Todd KH, Shete SS, Hanna EY. Survival patterns in squamous cell carcinoma of the head and neck: pain as an independent prognostic factor for survival. J Pain. 2014 Oct;15(10):1015-22. doi: 10.1016/j.jpain.2014.07.003. Epub 2014 Jul 17. PMID: 25043982; PMCID: PMC4418559.

Rosen RD, Sapra A. TNM Classification. [Updated 2022 Feb 17]. In: StatPearls [Internet]. Treasure Island (FL): StatPearls Publishing; 2022 Jan-. Available from: https://www.ncbi.nlm.nih.gov/books/NBK553187/

Siddiqui F, Vaqar S, Siddiqui AH. Lung Cancer. [Updated 2022 May 5]. In: StatPearls [Internet]. Treasure Island (FL): StatPearls Publishing; 2022 Jan-. Available from: https://www.ncbi.nlm.nih.gov/books/NBK482357/

Siegel RL, Miller KD, Fuchs HE, Jemal A. Cancer statistics, 2022. CA Cancer J Clin. 2022 Jan;72(1):7-33. doi: 10.3322/caac.21708. Epub 2022 Jan 12. PMID: 35020204. https://doi.org/10.3322/caac.21708

Souers, A., Leverson, J., Boghaert, E. *et al.* ABT-199, a potent and selective BCL-2 inhibitor, achieves antitumor activity while sparing platelets. *Nat Med* **19**, 202–208 (2013). https://doi.org/10.1038/nm.3048

Tai Q, Zhang L, Hu X. Clinical characteristics and treatments of large cell lung carcinoma: a retrospective study using SEER data. Transl Cancer Res. 2020 Mar;9(3):1455-1464. doi: 10.21037/tcr.2020.01.40. PMID: 35117493; PMCID: PMC8799166.

Tao ZF, Hasvold L, Wang L, Wang X, Petros AM, Park CH, Boghaert ER, Catron ND, Chen J, Colman PM, Czabotar PE, Deshayes K, Fairbrother WJ, Flygare JA,

Hymowitz SG, Jin S, Judge RA, Koehler MF, Kovar PJ, Lessene G, Mitten MJ, Ndubaku CO, Nimmer P, Purkey HE, Oleksijew A, Phillips DC, Sleebs BE, Smith BJ, Smith ML, Tahir SK, Watson KG, Xiao Y, Xue J, Zhang H, Zobel K, Rosenberg SH, Tse C, Leverson JD, Elmore SW, Souers AJ. Discovery of a Potent and Selective BCL-XL Inhibitor with in Vivo Activity. ACS Med Chem Lett. 2014 Aug 26;5(10):1088-93. doi: 10.1021/ml5001867. PMID: 25313317; PMCID: PMC4190639.

van Deursen JM. The role of senescent cells in ageing. Nature. 2014 May 22;509(7501):439-46. doi: 10.1038/nature13193. PMID: 24848057; PMCID: PMC4214092.

Vellanki PJ, Mulkey F, Jaigirdar AA, Rodriguez L, Wang Y, Xu Y, Zhao H, Liu J, Howe G, Wang J, Choo Q, Golding SJ, Mansell V, Korsah K, Spillman D, de Claro RA, Pazdur R, Beaver JA, Singh H. FDA Approval Summary: Nivolumab with I pilimumab and Chemotherapy for Metastatic Non-small Cell Lung Cancer, A Collaborative Project Orbis Review. Clin Cancer Res. 2021 Jul 1;27(13):3522-3527. doi: 10.1158/1078-0432.CCR-20-4338. Epub 2021 Feb 25. PMID: 3 3632925; PMCID: PMC8254731.

Vigneswaran N, Williams MD. Epidemiologic trends in head and neck cancer and aids in diagnosis. Oral Maxillofac Surg Clin North Am. 2014 May;26(2):123-41. doi: 10.1016/j.coms.2014.01.001. PMID: 24794262; PMCID: PMC4040236.

Wong, R.S. Apoptosis in cancer: from pathogenesis to treatment. *J Exp Clin Cancer Res* **30**, 87 (2011). https://doi.org/10.1186/1756-9966-30-87

Yanumula A, Cusick JK. Biochemistry, Extrinsic Pathway of Apoptosis. [Updated 2022 Aug 1]. In: StatPearls [Internet]. Treasure Island (FL): StatPearls Publishing; 2022 Jan-. Available from: https://www.ncbi.nlm.nih.gov/books/NBK560811/

Zappa C, Mousa SA. Non-small cell lung cancer: current treatment and future advances. Transl Lung Cancer Res. 2016 Jun;5(3):288-300. doi: 10.21037/tlcr.2016.06.07. PMID: 27413711; PMCID: PMC4931124.